CLM - R 67

CLM - R 67

United Kingdom Atomic Energy Authority

RESEARCH GROUP

Report

BEHAVIOR OF CHARGED PARTICLES IN A TOROIDAL MAGNETIC FIELD

KOJI UO

Culham Laboratory
Abingdon Berkshire

1966

Available from H. M. Stationery Office

SIX SHILLINGS NET

U.D.C.
533.95
621.039.623

UNCLASSIFIED
(Approved for sale)

CLM - R67

BEHAVIOR OF CHARGED PARTICLES IN A TOROIDAL MAGNETIC FIELD

by

KOJI UO

ABSTRACT

The motion of a charged particle in a Tokomak type magnetic field is analysed. By using the φ-component of the canonical angular momentum in the toroidal coordinate system (r, θ, φ) and the total energy as the constants of motion, the region of allowed particle motion has been calculated. This region is given by a function of the φ-component of the magnetic vector potential A_φ, the vertical magnetic field, the electric field and the initial position and motion of the particle. Then the allowable range of energy and velocity of the particle to be confined within a limiting surface is determined. For given initial position of the particle, the maximum energy of the confined particle shows strong dependence on $\Upsilon \equiv (v_\varphi)\text{initial}/v$, and strong asymmetry on the sign of Υ. The energy and the velocity distributions of the confined particles have strong radial dependence. In the region near the limiting surface, almost uni-direction φ-motion is allowed for ions. This stems from the fact that the θ-component of the magnetic field is the effective agent for single particle confinement in the toroidal system. The effect of the vertical and radial electric field is discussed. The former electric field is unfavourable for the particle confinement and the latter favourable.

UKAEA Research Group,
Culham Laboratory,
Nr. Abingdon,
Berks.

September, 1966 (C/18 DS)

C O N T E N T S

		Page
1.	INTRODUCTION	1
2.	THE TOROIDAL MAGNETIC FIELD	2
3.	THE CHARGED PARTICLE MOTION IN A TOROIDAL MAGNETIC FIELD WITH ROTATIONAL TRANSFORM	5
4.	PARTICLE LOSS	15
5.	THE CHARGED PARTICLE MOTION IN A TOROIDAL MAGNETIC FIELD WITH ROTATIONAL TRANSFORM AND ELECTRIC FIELD	18
6.	TRAPPED PARTICLES BY THE MIRROR EFFECT	23
7.	GUIDING CENTRE LIMIT MODEL	23
	ACKNOWLEDGMENTS	24
	REFERENCES	25

1. INTRODUCTION

Under the assumptions of magnetohydrodynamics, the necessary condition of plasma equilibrium is given by

$$\nabla p = \underline{J} \times \underline{B} \qquad \ldots (1)$$

where p is the plasma pressure. $\underline{J}$ the plasma current density and $\underline{B}$ the magnetic flux density. From eq.(1), it is concluded that the equi-pressure surfaces of the plasma are woven by the magnetic lines of force and the stream line of the plasma current. A topological consideration of eq.(1) shows that such an equi-pressure surface should be toroidal. For the rotationally transformed magnetic field, the equi-pressure surface should coincide with the magnetic surface of the field.

However, the charged particles in the toroidal magnetic field do not move exactly along the lines of force. These particles are affected by many forces: the Lorenz force, the centrifugal force, the Coriolis force, the magnetic field gradient force and the electric field force. The real surface along which the charged particles move, namely the so-called drift surface[3], is different from the magnetic surface, and is not the same for ions as for electrons. These differences result in the building up of electric fields in the plasma. If the resultant electric field coincides with the initially given electric field there will be a self-consistent solution of the equilibrium.

The first step in the solution of this problem, in this paper, is an investigation of the region where the charged particle motion is allowed in the toroidal magnetic field, and this can be done in three ways. The first method is to obtain a solution for the particle orbit by using the equation of motion of the particle directly. The second is to investigate the orbit of the guiding centre of the particle by using adiabatic invariants[1,2,3]. The third is to define the region of the allowable particle motion by using the φ-component of the canonical angular momentum as a constant of motion[4,5].

Although the first method gives a short time visual picture of the real particle orbit for given initial condition and field parameters, it needs computer calculation in general since it is very difficult to obtain the analytic solution of the equation of motion. Since the computer cannot be run in infinite time, there is always some uncertainty. The second method is applicable for almost any kind of magnetic field, and yields an analytic solution. However, it is inapplicable for non-adiabatic particles. Although the third method is applicable only for the case in which the fields have symmetry about the major radius, it

gives simple analytic solutions of the region in which the particle motion is allowed and is applicable for non-adiabatic particles.

In this paper the third method is used to investigate the allowable region of the particle motion in a Tokomak type[6,7,8] magnetic field. The region is given as a function of azimuthal and vertical magnetic induction, the major and the minor radii of the toroidal plasma, the initial value of the particle kinetic energy, the vertical and the radial electric field intensity, the initial position of the particle and the initial value of the ratio of the longitudinal component of the particle velocity $v_{\varphi 1}$ to the square root of the initial total energy. This region will give us a close picture of the particle drift surface.

The condition for particle confinement is that the allowable region for particle motion should be inside the limiting surface which limits the plasma column diameter. Then, we draw the diagram of maximum energy of the confined particle with respect to $\gamma = \frac{v_{\varphi 1}}{\sqrt{\frac{2}{m}H}}$, where H is the Hamiltonian, and to the initial position of the particle for given field parameters. This diagram is a monotonically increasing function of γ, and has strong dependence on γ.

The effect of the electric field is discussed. We take two electric fields, i.e. the radial electric field due to the radial charge separation and the vertical electric field due to the vertical charge separation resulting from the u-bend drift and finite conductivity of the plasma. It is proved that the former electric field is favourable for particle confinement and the latter unfavourable.

2. THE TOROIDAL MAGNETIC FIELD

Assume a magnetic field similar to that of Tokomak, where the axial magnetic field is given by

$$\underline{B}_a = \underline{e}_\varphi B_o \frac{1}{\eta} , \qquad \ldots (2)$$

where

$$\eta = \eta(r,\theta) = 1 + \frac{r}{R}\cos\theta . \qquad \ldots (3)$$

The toroidal coordinate system (r,θ,φ) is used throughout the analysis except where, on one occasion the cylindrical coordinate system (ρ,φ,z) is used for convenience. The relations between these coordinate systems and the direction of the magnetic field and current are shown in Fig.1. The helical magnetic field of Tokomak is produced by the ohmic

heating current the density of which is given by

$$\underline{J} = \underline{e}_\varphi \frac{i_o}{\eta} = \underline{e}_\varphi \frac{\sigma V_L}{2\pi R} \frac{1}{\eta} , \qquad \cdots (4)$$

where σ is the conductivity of the plasma, V_L the loop voltage of the ohmic heating. The azimuthal magnetic field produced by $\underline{J}$ should satisfy the relation

$$\underline{\nabla} \times \underline{B}_h = \underline{\nabla} \times \underline{\nabla} \times \underline{A}_h = \mu_o \underline{J} , \qquad \cdots (5)$$

where $\underline{A}_h$ is the vector potential of the field produced by $\underline{J}$. Assuming that

$$\frac{\partial}{\partial \varphi} \equiv 0 , \qquad \cdots (6)$$

eqs.(4) and (5) yield

$$\frac{\partial^2 A'_\varphi}{\partial r^2} + \left(\frac{1}{r} + \frac{\cos\theta}{R} \right) \frac{\partial A'_\varphi}{\partial r} + \frac{1}{r^2} \frac{\partial^2 A'_\varphi}{\partial \theta^2} - \frac{\sin\theta}{\eta R} \frac{\partial A'_\varphi}{r \partial \theta} - \frac{A'_\varphi}{\eta^2 R^2} = \mu_o \frac{i_o}{\eta} , \qquad \cdots (7)$$

where A'_φ is the φ-component of $\underline{A}_h$. Solving the above equation we obtain to good approximation

$$\underline{A}_h = \underline{e}_\varphi A'_\varphi = \underline{e}_\varphi \frac{F(r,\theta)}{\eta} , \qquad \cdots (8)$$

where

$$\begin{aligned} F(r,\theta) &= -\frac{B_1}{2r_o} r^2 \, Q(r,\theta) \\ &= -\frac{B_1}{2r_o} r^2 \left(1 + \frac{r}{4R} \cos\theta - \frac{1}{8} \frac{r^2}{R^2} \cos^2\theta + \frac{1}{32} \frac{r^2}{R^2} \right) \qquad \cdots (9) \end{aligned}$$

$$B_1 = \frac{\mu_o I_o}{2\pi r_o} , \quad I_o = \pi r_o^2 i_o \qquad \cdots (10)$$

where r_o is the radius of the plasma column or the limiter radius. This solution is valid up to the order of $(r/R)^2$. Then, the azimuthal field is given by

$$\begin{aligned} \underline{B}_h &= \underline{e}_r \frac{1}{\eta} \frac{\partial F}{\partial r} + \underline{e}_\theta \frac{1}{\eta} \frac{\partial F}{r \partial \theta} \\ &= \underline{e}_r \frac{B_1}{\eta} \frac{r^2}{8 R r_o} \sin\theta \left(1 - \frac{r}{R} \cos\theta \right) \\ &\quad + \underline{e}_\theta \frac{B_1}{\eta} \frac{r}{r_o} \left(1 + \frac{3r}{8R} \cos\theta - \frac{r^2}{4R^2} \cos^2\theta + \frac{1}{16} \frac{r^2}{R^2} \right) . \qquad \cdots (11) \end{aligned}$$

The vertical magnetic field, $\underline{B}_v$, for suppressing the magnetic surface shift due to the secondary current along the helical lines of force is given by

$$\underline{B}_v = \underline{e}_z (-B_v) . \qquad \cdots (12)$$

The vector potential of $\underline{B}_v$ is given by

$$\underline{A}_v = \underline{e}_\varphi \frac{S}{\eta} , \quad S = -\frac{1}{2} B_v R \eta^2 . \qquad \cdots (13)$$

The vector potential of the axial field $\underline{B}_a$ is given by

$$\underline{A}_a = \underline{e}_z \{ -B_o R \log (R\eta) \} . \qquad \cdots (14)$$

Thus the total vector potential of all magnetic field presented here is given by

$$\begin{aligned}\underline{A} &= \underline{e}_r A_r + \underline{e}_\theta A_\theta + \underline{e}_\varphi A_\varphi \\ &= \underline{e}_r B_o R \sin\theta \log(R\eta) + \underline{e}_\theta B_o R \cos\theta \log(R\eta) \\ &\quad + \underline{e}_\varphi \left(\frac{F}{\eta} + \frac{S}{\eta} \right) . \end{aligned} \qquad \cdots (15)$$

The equation of lines of force is given by solving the following differential equation;

$$\frac{dr}{B_r} = \frac{r d\theta}{B_\theta} = \frac{R\eta d\varphi}{B_\varphi} , \qquad \cdots (16)$$

where

$$\begin{aligned}\underline{B} &= \underline{B}_a + \underline{B}_h + \underline{B}_v \\ &= \underline{e}_r \frac{1}{\eta} \frac{\partial}{\partial r} (F+S) + \underline{e}_\theta \left\{ -\frac{1}{\eta} \frac{\partial}{r\partial\theta} (F+S) \right\} + \underline{e}_\varphi \frac{B_o}{\eta} . \end{aligned} \qquad \cdots (17)$$

The solution of eq.(16) is given by

$$F(r, \theta) + S(r, \theta) = \text{const.} \qquad \cdots (18)$$

Solving eq.(18) with respect to r yields the equation of the magnetic surface

$$\begin{aligned}\frac{r}{r_o} &= \left[\left\{ w + \frac{\varepsilon^2}{32} w^2 + \frac{\varepsilon^2}{4} \cos^2\theta \left(4\mu^2 - \frac{11}{16} w^2 + 3\mu w \right) \right\}^{\frac{1}{2}} - \frac{\varepsilon}{8} \cos\theta \, (w + 8\mu) \right] \\ &\quad \times \left\{ 1 + \frac{\varepsilon^2}{32} w + \frac{\varepsilon^2}{4} \cos^2\theta \left(2\mu - \frac{3}{4} w \right) \right\}^{-1} , \end{aligned} \qquad \cdots (19)$$

where

$$w = s^2 Q_1 + \mu (\eta_1^2 - 1) , \qquad \cdots (20)$$

$$\left.\begin{aligned} &\varepsilon = \frac{r_o}{R} , \quad \mu = \frac{B_v}{B_1} \frac{1}{\varepsilon} , \\ &s = \frac{r_1}{r_o} , \quad \eta_1 = \eta(r_1, 0) = 1 + \varepsilon s , \\ &Q_1 = Q(r_1, 0) = 1 + \frac{\varepsilon}{4} s - \frac{3}{32} \varepsilon^2 s^2 . \end{aligned}\right\} \qquad \cdots (21)$$

r_1 is the value of r on the magnetic surface for $\theta = 0$. Therefore we can use s as the parameter which discriminates the magnetic surfaces from each other. Here, we allow negative values for s and r. Negative s means that, for $\theta = 0$, $r = s r_o < 0$. In this case, r should be measured in the opposite direction to the normal r direction. By this means, we can avoid using the double sign, $\pm$, in front of the root. When the value inside the root becomes negative for some range of θ, the magnetic surface does

not exist in the range. The expression (19) is valid up to the order of ε^2. Naturally, $r/r_0 = s$ for $\theta = 0$, which can be shown by expanding eq.(19) carefully.

Taking the special case when $s = 0$. We have

$$\frac{r}{r_0} = \frac{\mu\varepsilon\{|\cos\theta| - \cos\theta\}}{1 + \frac{\varepsilon^2}{2}\mu\cos^2\theta} \qquad \ldots (22)$$

$$\left.\begin{array}{lll} \text{For} & \cos\theta \geqslant 0 \quad , & \dfrac{r}{r_0} = 0 \ , \\ \text{for} & \cos\theta < 0 \quad , & \dfrac{r}{r_0} = -\dfrac{2\varepsilon\mu\cos\theta}{1 + \frac{\varepsilon^2}{2}\mu\cos^2\theta} \end{array}\right\} \qquad \ldots (23)$$

Thus the entire magnetic surface is in the range, $\frac{\pi}{2} \leqslant \theta \leqslant \frac{3\pi}{2}$. Therefore, the magnetic axis will exist inside the above magnetic surface. Clearly, the parameter of the magnetic axis, s_0, is negative and is obtained by using the condition making the value inside the root in eq. (19) zero for $\theta = \pi$. Using this condition we obtain the parameter of magnetic axis

$$s_0 \approx -\frac{\varepsilon\mu}{1 + \frac{1}{2}\varepsilon^2\mu} \approx -\frac{B_V}{B_1} \qquad \ldots (24)$$

Thus, the position of the magnetic axis is given by

$$(r, \theta) = \left(\frac{\varepsilon\mu r_0}{1 + \frac{1}{2}\varepsilon^2\mu} \ , \ \pi\right) . \qquad \ldots (25)$$

This shift of the magnetic axis from the minor axis towards the major axis is the result of applying the vertical field $\underline{B}_V$. However, B_V/B_1 in the Tokomak field is a quantity of order ε. Therefore, the shift is very small in general. The magnetic surfaces and the magnetic axis are shown in Fig.2. The expression for $\underline{B}_V$ is shown in Appendix 1.

3. THE CHARGED PARTICLE MOTION IN A TOROIDAL MAGNETIC FIELD WITH ROTATIONAL TRANSFORM

Let us consider the permitted region for motion of the charged particle in the magnetic field given by eq. (17). The Lagrangian of the particle motion is given by

$$\begin{aligned} L &= \frac{m}{2}\underline{v}^2 + q\,\underline{v}.\underline{A} \\ &= \frac{m}{2}\{\dot{r}^2 + (r\dot{\theta})^2 + (R\eta\dot{\varphi})^2\} + q\{\dot{r}A_r + (r\dot{\theta})A_\theta + (R\eta\dot{\varphi})A_\varphi\} , \end{aligned} \qquad \ldots (26)$$

where m and q are the mass and the charge of the particle. The canonical angular momenta are given by

$$P_r = \frac{\partial L}{\partial \dot{r}} = m\dot{r} + q\,Ar\,,$$

$$P_\theta = \frac{\partial L}{\partial \dot{\theta}} = m r^2 \dot{\theta} + qr A_\theta\,, \qquad \ldots (27)$$

$$P_\varphi = \frac{\partial L}{\partial \dot{\varphi}} = m(R\eta)^2 \dot{\varphi} + q R \eta A_\varphi\,.$$

The Hamiltonian of the particle motion is

$$H = \dot{\underline{r}} \cdot \underline{P} - L$$

$$= \frac{m}{2}\left\{\dot{r}^2 + (r\dot{\theta})^2 + (R\eta\dot{\varphi})^2\right\} = \frac{m}{2} v^2\,,\ v > 0\,. \qquad \ldots (28)$$

Using eq.(27), we can write

$$H = \frac{1}{2m}\left\{(P_r - qA_r)^2 + \frac{1}{r^2}(P_\theta - qrA_\theta)^2 + \frac{1}{R^2\eta^2}(P_\varphi - qR\eta A_\varphi)^2\right\}. \qquad \ldots (29)$$

Since

$$\frac{dP_\varphi}{dt} = -\frac{\partial H}{\partial \varphi} = 0\,, \qquad \ldots (30)$$

the canonical angular momentum P_φ is a constant of motion. Note that the condition (30) stems from the perfect symmetry with respect to the major axis, and will not hold in the case of the Stellarator or other undulating field. The other constant of motion is the total kinetic energy, namely the Hamiltonian, since $dH/dt = \partial H/\partial t = 0$. Let

$$U = \frac{1}{2mR^2\eta^2}(P_\varphi - qR\eta A_\varphi)^2 = \frac{m}{2} V_\varphi^2\,, \qquad \ldots (31)$$

where $V_\varphi = R\eta\dot{\varphi}$. Since U is a function of position alone, U behaves as an equivalent potential. We can write

$$H = \frac{1}{2m}\left\{(P_r - qA_r)^2 + \frac{1}{r^2}(P_\theta - qrA_\theta)^2\right\} + U \qquad \ldots (32)$$

$$= \frac{m}{2}(v_r^2 + v_\theta^2) + U$$

The permitted range for the particle motion is determined by

$$U \leqslant H\,. \qquad \ldots (33)$$

Referring to eqs. (28) and (31), the above inequality simply means

$$v_\varphi^2 \leqslant v^2\,. \qquad \ldots (34)$$

This inequality yields

$$-1 \leqslant \Upsilon_o \leqslant 1 \quad , \quad \Upsilon_o = \frac{v_\varphi}{v} \ . \qquad \ldots (35)$$

Note that it is not always necessary for Υ_o to take all values between 1 and -1 . v in eq. (35) is the absolute velocity of the particle and $v \geqslant 0$. There are three categories of motion given by eq. (35) and indicated in Fig.3. They are: (a) the particle motion shown in curve A where v_φ takes all values between v and $-v$, and the motion is bounded between the two surfaces $r(\Upsilon_o = 1)$ and $r(\Upsilon_o = -1)$; (b) the particle motion shown in curve B where v_φ takes the value between v and $v_{\varphi m}$ and it does not take a smaller value than $v_{\varphi m}$. (In the case of curve B', the minimum value of v_φ is negative); (c) the particle motion shown in curve C where v_φ takes the values between $-v$ and $-v_{\varphi m}$. (In the case of curve C', the maximum of v_φ is positive.) However the motions typified by curves C and C' are not permitted for ions as shown later.

The equation

$$\Upsilon_o = \text{const} \qquad \ldots (36)$$

gives a surface on which v_φ takes a constant value $\Upsilon_o v$. Referring to eqs.(27) and (36) yields

$$\frac{v_{\varphi o}}{v} = \frac{P_\varphi - qR\eta A_\varphi}{mvR\eta} = \Upsilon_o = \text{const.} \qquad \ldots (37)$$

Let the initial condition of the particle

$$r = r_1 \quad , \quad \theta = 0 \quad , \quad \dot{\varphi} = \dot{\varphi}_1 \quad , \quad \sqrt{\dot{r}^2 + (r\dot{\theta})^2 + (R\eta\dot{\varphi})^2} = v \ . \qquad \ldots (38)$$

Substituting eq. (38) into eq. (27) we find

$$\frac{P_\varphi}{mRv} = \eta_1 \Upsilon - \frac{1}{\delta}\left(s^2 Q_1 + \mu \eta_1^{\,2}\right) , \qquad \ldots (39)$$

where

$$\left.\begin{aligned} \Upsilon &= \frac{v_{\varphi 1}}{v} = \frac{R\eta_1 \dot{\varphi}_1}{v} \ , \\ \delta &= \frac{2v}{\omega_1 r_o} \quad , \quad \omega_1 = \frac{q\mathcal{B}_1}{m} \ . \end{aligned}\right\} \qquad \ldots (40)$$

Considering only ions (electrons will be discussed later) and substituting eqs. (3),(9) (13), (15), (21), and (39) into eq. (37), and solving (37) with respect to r, we have approximately

$$r(\Upsilon_0) = \frac{r_0}{1+\frac{\varepsilon^2}{32} w_0 + \frac{\varepsilon^2}{4}\cos^2\theta\,(\Upsilon_0\delta + 2\mu - \frac{3}{4} w_0)} \times \left(\left[w_0 + \frac{\varepsilon^2}{32} w_0^2 + \frac{\varepsilon^2}{4}\cos^2\theta \left\{ (\Upsilon_0\delta - 2\mu)^2 + w_0 \left(\frac{\Upsilon_0\delta}{2} - \frac{11}{16} w_0 + 3\mu \right) \right\} \right]^{\frac{1}{2}} + \frac{\varepsilon}{8}\cos\theta \left\{ 4(\Upsilon_0\delta - 2\mu) - w_0 \right\} \right) . \quad \ldots (41)$$

where

$$w_0 = s^2 Q_1 + \mu\,(\eta_1^2 - 1) + \delta\,(\Upsilon_0 - \eta_1 \Upsilon) . \quad \ldots (42)$$

This is the equation of the surface on which $v_\varphi = \Upsilon_0 v$ and is valid up to the order of ε^2. δ is proportional to the square root of the particle kinetic energy. If $\delta = 0$, (41) reduces to (19), the equation of the magnetic surface. As in the case of eq. (19), we allow r to take a negative value. When the value inside the root in eq. (41) becomes negative for some range of θ, the surface, on which $v_\varphi = \Upsilon_0 v$, does not exist in the range. If the value inside the root is negative for all values of θ, v_φ cannot take the value $\Upsilon_0 v$. Whether v_φ can take the value $\Upsilon_0 v$ or not is simply determined by the initial conditions v, Υ and s for given field parameters such as ε, μ and ω_1. When δ is larger than $s^2 Q_1 + \mu(\eta_1^2 - 1)$, the sign of w_0 depends mainly on the sign of $\Upsilon_0 - \eta_1 \Upsilon$. Therefore, the initial condition $\Upsilon = -1$ yields the maximum freedom to the allowable value of v_φ. On the contrary, $\Upsilon = 1$ yields the minimum. The particle can take the state $\Upsilon_0 = 1$ for all values of Υ. However, it is not always possible for the particle to take the state $\Upsilon_0 = -1$. For instance, when $\Upsilon \geqslant 0$, the very low energy particle alone, namely a small δ particle, can take the state $\Upsilon_0 = -1$. For given value of Υ, $r(\Upsilon_0)$ takes its maximum value when $\Upsilon_0 = 1$. On the surface $r(\Upsilon_0 = 1)$, v_φ becomes v, the maximum value of v_φ, and $\sqrt{v_r^2 + v_\theta^2}$ becomes zero. Therefore, the particle cannot escape from the region surrounded by the surface

$$r(\Upsilon_0 = 1) = \frac{r_0}{1+\frac{\varepsilon^2}{32} w_1 + \frac{\varepsilon^2}{4}\cos^2\theta\,(\delta + 2\mu - \frac{3}{4} w_1)} \times \left(\left[w_1 + \frac{\varepsilon^2}{32} w_1^2 + \frac{\varepsilon^2}{4}\cos^2\theta \left\{ (\delta - 2\mu)^2 + w_1 \left(\frac{\delta}{2} - \frac{11}{16} w_1 + 3\mu \right) \right\} \right]^{\frac{1}{2}} + \frac{\varepsilon}{8}\cos\theta \left\{ 4(\delta - 2\mu) - w_1 \right\} \right) . \quad \ldots (43)$$

where

$$w_1 = s^2 Q_1 + \mu(\eta_1^2 - 1) + \delta\ (1 - \eta_1 \Upsilon)\ . \qquad \ldots (44)$$

This is the upper boundary surface. The particle motion is restricted inside this surface. We can prove that $r = r(\Upsilon_0 = 1)$ cannot become infinite for finite δ.

When the value inside the root in eq. (41) is not negative, the particle motion has an additional restriction, the lower boundary surface on which $\Upsilon_0 = -1$, namely $v_\varphi = -v$. In this case the particle motion is restricted inside the region between the upper and the lower boundary surfaces. The latter is given by

$$r(\Upsilon_0 = -1) = -\frac{r_0}{1 + \frac{\varepsilon^2}{32} w_2 + \frac{\varepsilon^2}{4} \cos^2\theta \left(-\delta + 2\mu - \frac{3}{4} w_2\right)}$$

$$\times \left(\left[w_2 + \frac{\varepsilon^2}{32} w_2^2 + \frac{\varepsilon^2}{4} \cos^2\theta \left\{ (\delta + 2\mu)^2 + w_2 \left(-\frac{\delta}{2} - \frac{11}{16} w_2 + 3\mu \right) \right\} \right]^{\frac{1}{2}} \right.$$

$$\left. - \frac{\varepsilon}{8} \cos\theta \left\{ 4\ (\delta + 2\mu) + w_2 \right\} \right), \qquad \ldots (45)$$

where

$$w_2 = s^2 Q_1 + \mu\ (\eta_1^2 - 1) - \delta\ (1 + \eta_1 \Upsilon)\ . \qquad \ldots (46)$$

Now, let us investigate the motion of the charged particle for different initial conditions of Υ and s. The therm UBS is used to denote the upper boundary surface, $r = r(\Upsilon_0 = 1)$, and LBS the lower boundary surface, $r = r(\Upsilon_0 = -1)$.

Case 1. $\Upsilon = 1$

In this case w_1 and w_2 become

$$\left.\begin{aligned} w_1 &= s^2 Q_1 + \varepsilon s \mu\ (2 + \varepsilon s) - \varepsilon s \delta \\ w_2 &= s^2 Q_1 + \varepsilon s \mu\ (2 + \varepsilon s) - \delta(1 + \eta_1)\ . \end{aligned}\right\} \qquad \ldots (47)$$

Let

$$\left.\begin{aligned} D_1(\theta) &= w_1 + \frac{\varepsilon^2}{32} w_1^2 + \frac{\varepsilon^2}{4} \cos^2\theta \left\{ (\delta - 2\mu)^2 + w_1 \left(\frac{\delta}{2} - \frac{11}{6} w_1 + 3\mu \right) \right\}, \\ D_2(\theta) &= w_2 + \frac{\varepsilon^2}{32} w_2^2 + \frac{\varepsilon^2}{4} \cos^2\theta \left\{ (\delta + 2\mu)^2 + w_2 \left(-\frac{\delta}{2} - \frac{11}{16} w_2 + 3\mu \right) \right\}. \end{aligned}\right\} \qquad \ldots (48)$$

Case 1a $\Upsilon = 1\ ,\ s > 0$

(i) $D_1(\theta) > 0\ ,\ D_2(\theta) > 0$ for all θ value.

When δ is so small that D_1 and D_2 are positive for all values of θ, UBS and LBS both exist as shown in Fig.4. The particle motion is limited in the region between UBS

and LBS. First, we discuss the case that $B_a = 0$. Since, $\Upsilon = v_{\varphi_1}/v = 1$ initially, $\sqrt{v_r^2 + v_\theta^2} = 0$ initially. The Lorenz force $v \times (B_h + B_v)$ is acting in the $\rho - \varphi$ plane. Then, the particle motion is restricted to the plane $P_1 P_2$ as shown in Fig.4. The real particle orbit is shown by the curve a in Fig 6. $\Upsilon_0 = v_\varphi/v$ can take the values of ± 1. This is the category (a) motion in Fig.3.

(ii) $$D_1(\theta) > o \quad , \quad D_2(\theta) < o \quad \text{for all} \quad \theta \quad \text{value.}$$

when δ is not too large so that we can keep $D_1 > o$ and δ is large enough so that $D_2 < o$, LBS does not exist, but UBS does, as shown in Fig.5. The particle motion is limited inside UBS, and without $\underline{B}_a$, it is restricted to the plane $P_1 P_2$. The real particle orbit is shown by the curve b in Fig.6. Υ_0 can take only positive values. This is the category (b) motion shown in Fig.3. Particles of category (a) have negative net v_φ velocity and, those of (b) have positive. The motion depended by curve B' in Fig.3 is shown in the curve b'in Fig.6. In this case, the net v_φ velocity is positive for larger δ and negative for smaller δ. These dissimilarities stem from the difference in particle energy.

The presence of the axial field $\underline{B}_a$ adds to the particle motion a fine gyration around the particle path shown in Fig.6. Also, the effect of the U-bend drift, namely the sum of the curvature drift and the gradient drift, results in a rotational motion of the particle around the minor axis. The curves shown in Fig.6 rotate around the minor axis as shown in Figs. 4 and 5. Thus the particle orbit consists of three kinds of spirals for the category (a) motion. It is similar to the orbit of the moon with respect to the circular orbital motion of the sun. However, the permitted region of particle motion is still restricted between UBS and LBS or inside UBS.

The axial field $\underline{B}_a$ has no effect on the permitted region of particle motion, because the position where $|v_\varphi|$ takes its maximum value v is determined only by the vector potential A_φ, namely B_h and B_v, and not by B_a. Since $(v_r^2 + v_\theta^2)$ becomes zero when the particle is at the turning point of the motion in the r direction (see eqs. (27),(28) and (42)),the particle cannot escape from the region bounded by UBS and LBS. The effect of the adiabatic invariants provides a further restriction on the region. However, the essential feature of the region will remain unchanged.

(iii)
$$\left.\begin{aligned} &D_1(\theta) \geqslant o \quad \text{for} \quad \cos^2\theta \geqslant \cos^2\theta_0 \,, \\ &D_1(\theta) < o \quad \text{for} \quad \cos^2\theta < \cos^2\theta_0 \,, \\ &D_2(\theta) < o \quad \text{for all} \quad \theta \quad \text{value.} \end{aligned}\right\} \qquad \ldots (49)$$

This situation will happen when $w_1 < o$. From eq. (47), we can see this is the case for large δ. In this case, LBS does not exist, and UBS is shown in Fig.7. Note that a negative value is allowed for r. In this case, UBS exists only for $-\frac{\pi}{2} \leqslant \theta \leqslant \frac{\pi}{2}$. In the case without $\underline{B}_a$, the motion is restricted to the plane P_1P_2 as shown in Figs 7 and 8. This is the category (b) motion of Fig.3. The center of curvature of the orbit is always inside the curve of the orbit. The particle starts from the point A_1 on UBS with the initial condition $\Upsilon = 1$, and turns the orbit towards the minor axis under the effect of $\underline{B}_h$ and $\underline{B}_v$. Since $B_v << B_h$ and B_h becomes small towards the minor axis, the curvature of the orbit becomes small and takes its minimum value at the point A_2 on LBS. After reaching the point A_2, the particle moves away from the minor axis into the region of stronger B_h increasing the curvature of its orbit. Thus, it continues its motion on the plane P_1P_2. The presence of $\underline{B}_a$, as in the discussion given in (i) and (ii), deforms the orbit. However, the region of motion is still restricted inside UBS as shown in Fig.7. In this case, the particle orbit is completely outside the minor axis.

When $\theta_o = \frac{\pi}{2}$, P_2 in Fig 7 coincides with the minor axis. This is the transit situation between the upper boundary surfaces in Fig.5 and Fig.7. In this case, $w_1 = o$.

When $\theta_o = O$, UBS shown in Fig.7 degenerates to a circle, and the particle maintains a circular motion along this circle around the major axis. The radius of this circle is given by $R + r_o s_o$ and s_o is given by

$$s_o \cong \frac{\varepsilon}{2} \frac{\delta - 2\mu}{1 + \frac{\varepsilon^2}{16}(3\delta + 10\mu)} \quad . \qquad \ldots (50)$$

In this case, the centrifugal force of this circular motion is just balanced by the Lorenz force.

Case 1b $\Upsilon = 1$, $s = o$.

In this case, from eq. (47) we have $w_1 = o$ and $w_2 < o$. LBS does not exist and UBS is given by

$$r(\Upsilon_o = 1) = r_o \frac{\frac{\varepsilon}{2}\{|(\delta - 2\mu)\cos\theta| + (\delta - 2\mu)\cos\theta\}}{1 + \frac{\varepsilon^2}{4}\cos^2\theta(\delta + 2\mu)} \qquad \ldots (51)$$

Since $w_1 = o$, this case coincides with the case mentioned in (iii) above for $\theta_o = \frac{\pi}{2}$. Let us investigate this in a little more detail.

(i) $\delta > 2\mu$

Equation (51) becomes,

$$\left.\begin{aligned} &\text{for } -\frac{\pi}{2} \leqslant \theta \leqslant \frac{\pi}{2} \quad , \qquad r(\Upsilon_0 = 1) = \frac{r_0 \varepsilon (\delta - 2\mu) \cos\theta}{1 + \frac{\varepsilon^2}{4} \cos^2\theta (\delta + 2\mu)} \quad , \\ &\text{for } \frac{\pi}{2} < \theta < \frac{3\pi}{2} \quad , \qquad r(\Upsilon_0 = 1) = 0 \quad . \end{aligned}\right\} \quad \ldots (52)$$

UBS is shown in Fig.7 by making the point P_2 coincide with the minor axis. The feature of the particle orbit is similar to Fig.8. The inside edge of UBS coincides with the minor axis, and the initial position is on the minor axis.

(ii) $\delta = 2\mu$

In this case, UBS degenerates to the minor axis, $r = 0$. Since $\underline{B}_h = 0$ on the minor axis, the centrifugal force v^2/R is balanced by the Lorenz force $-vB_v$ and the particle keeps its circular motion along the minor axis. $\delta = 2\mu$ just expresses the condition of the force balance.

(iii) $\delta < 2\mu$

Allowing the negative value of r, UBS is given by eq. (52), and is shown in Fig.9. UBS exists only for $\frac{\pi}{2} \leqslant \theta \leqslant \frac{3\pi}{2}$. The particle orbit is shown in Fig.10. The particle starts from the point on the axis A_2 with the velocity $\Upsilon = 1$, namely $v_\varphi = v$, $v_\Upsilon = v_\theta = 0$. Since $\underline{B}_h = 0$ on the axis, the particle moves away from the axis under the effect of $\underline{B}_v$. As the particle moves B_h increases and the curvature of the orbit decreases. After arriving at the point A_2, the particle starts to move towards the minor axis, thus continuing its periodic motion. This is the category (b) motion.

Case 1c $\Upsilon = 1$, $s < 0$.

In this case, the features of UBS, LBS and the particle orbits are similar to those in Figs 4, 5, 6, 9 and 10. This is seen by changing the initial position to the nearest edge of UBS. For the category (a) motion in Fig.6, the position of the curve should be transfered to the region, $\frac{\pi}{2} < \theta < \frac{3\pi}{2}$, namely the opposite side of the minor axis. However, the presence of $\underline{B}_a$ makes both cases similar.

Case 2 $\Upsilon = 0$

$$\left.\begin{aligned} w_1 &= s^2 Q_1 + \varepsilon s\mu(2 + \varepsilon s) + \delta \quad , \\ w_2 &= s^2 Q_1 + \varepsilon s\mu(2 + \varepsilon s) - \delta \quad . \end{aligned}\right\} \quad \ldots (53)$$

The features of UBS and LBS are similar to those in Figs.4 and 5. The particle orbits are shown in the curves b' and a in Fig.6. These correspond to the curves B'

and A in Fig.3. In this case, the initial position of the particle is at the point where $\Upsilon_0 = o$, namely $v_\varphi = o$. The category (b) motion is not allowed for this initial condition, $\Upsilon = o$.

Case 3a $\Upsilon = -1$, $s > o$.

$$\left.\begin{aligned} w_1 &= s^2 Q_1 + \varepsilon s\mu (2+\varepsilon s) + \delta(1+\eta_1) , \\ w_2 &= s^2 Q_1 + \varepsilon s \mu(2+\varepsilon s) + \varepsilon s\delta . \end{aligned}\right\} \quad \ldots (54)$$

Since $w_1 > o$ and $w_2 > o$, UBS and LBS both exist. This is the category (a) motion shown in Fig.3. UBS and LBS are similar to Fig.5 and the particle orbit is shown in curve a in Fig.6. The initial position is on LBS where $\Upsilon_0 = -1$. Although category (a) motion is allowed only for small δ particles in the case of $\Upsilon = 1$, it is allowed for all value of δ in this case unless the orbit crosses the limiting surface $r = r_0$.

Case 3b $\Upsilon = -1$, $s = o$.

$$w_1 = 2\delta \quad , \quad w_2 = o . \quad \ldots (55)$$

LBS is given by

$$\left.\begin{aligned} &\text{for } \frac{\pi}{2} > \theta > -\frac{\pi}{2} \quad , \quad r(\Upsilon_0 = -1) = o , \\ &\text{for } \frac{\pi}{2} \leqslant \theta \leqslant \frac{3\pi}{2} \quad , \quad r(\Upsilon_0 = -1) = \frac{\varepsilon \cos\theta(\delta + 2\mu)}{1 - \frac{\varepsilon^2}{4}\cos^2\theta(\delta - 2\mu)} \leqslant o \end{aligned}\right\} \quad \ldots (56)$$

UBS and LBS are shown in Fig.11. This is the category (a) motion and the particle orbit is similar to the curve a in Fig.6, making the points, where $\Upsilon_0 = -1$, to coincide with the minor axis. The initial position is on the minor axis. This is the category (a) motion.

Case 3c $\Upsilon = -1$, $s < o$.

(i) $$D_1(\theta) > o \text{ and } D_2(\theta) > o$$

Being contrary to the case of $\Upsilon = 1$, the above condition is satisfied for almost all value of δ except for extremely small δ . In this case, we have the category (a) motion. UBS and LBS are shown in Fig.12. This is the same case as Fig.4; the difference is only the initial position and velocity. The particle orbit is shown in the curve a in Fig.13. This is the category (a) motion. This motion has net negative v_φ . When $|s|$ is so small that $D_2(\theta) \geqslant o$ for $\cos^2\theta \geqslant \cos^2\theta_0$, LBS exists only for $\frac{\pi}{2} < \theta < \frac{3\pi}{2}$. UBS and LBS are shown in Fig.14. The orbit in this case is shown in

curve a' in Fig.13. Since s is small enough, $|B_v| > |B_h|$. Then the direction of gyration is opposite to that of the curve a. After entering the region $o \leqslant \theta \leqslant \frac{\pi}{2}$, Υ_o becomes 1 and the particle turns back into the region $\frac{\pi}{2} < \theta < \frac{3\pi}{2}$ again. Thus it continues its periodic motion. The same situation will occur as in Case 1a(i). The initial condition, $\Upsilon = -1$, means the existence of LBS. Therefore, $D_2(\theta)$ cannot be negative. Thus, in this case, the category (a) motion alone is allowed.

For the case of the initial condition, $\Upsilon = -1$, the initial position of the particle is on LBS. On the contrary, for the case of the initial condition, $\Upsilon = 1$, the initial position of the particle is on UBS. For particles having $\Upsilon = 1$, the motion outside UBS is inhibited. On the other hand, for particles having $\Upsilon = -1$, the particle moves away from LBS until it reaches UBS. Therefore, if the limiting surface, $r = r_o$, is considered, confinement is better for particles having $\Upsilon = 1$ than those having $\Upsilon = -1$. In general, the particle confinement is a monotonically increasing function of Υ as shown in the next section.

As mentioned before, the net velocity of v_φ, namely $\bar{v}_\varphi$, is negative for category (a) motion. On the other hand it is positive for category (b) motion. In the case of the curve B' (Fig.3) where $-1 < \Upsilon_o \leqslant o$ during the motion, $\bar{v}_\varphi$ is positive for larger δ and negative for smaller δ as shown in Fig.6. Generally speaking, $\bar{v}_\varphi > o$ for large δ and $\bar{v}_\varphi < o$ for small δ. This feature is related to the presence of an additional longitudinal current in the confined plasma.

In this section the discussion has been confined to ions. (Up to eq.(37) the discussion is valid for ions and electrons). Since the electric charge q is negative for electrons, ω_1 and δ in eq.(40) becomes negative. So the UBS for electrons is given by $r = r(\Upsilon_o = -1)$ and LBS by $r = r(\Upsilon_o = 1)$.

Putting $\delta = \delta_e < o$ in eqs (45) and (46) gives the UBS for electrons:

$$(UBS)_e = r(\Upsilon_o = -1) = \frac{r_o}{1 + \frac{\varepsilon^2}{32} w_2 + \frac{\varepsilon^2}{4} \cos^2\theta (|\delta_e| + 2\mu - \frac{3}{4} w_2)} \times \left(\left[w_2 + \frac{\varepsilon^2}{32} w_2^2 + \frac{\varepsilon^2}{4} \cos^2\theta \left\{ (|\delta_e| - 2\mu)^2 + w_2 \left(\frac{|\delta_e|}{2} - \frac{11}{16} w_2 + 3\mu \right) \right\} \right]^{\frac{1}{2}} + \frac{\varepsilon}{8} \cos\theta \left\{ 4 (|\delta_e| - 2\mu) - w_2 \right\} , \quad \ldots (57)$$

where

$$w_2 = s^2 Q_1 + \mu (\eta_1^2 - 1) + |\delta_e| (1 + \eta_1 \Upsilon) , \quad \ldots (58)$$

$$\delta_e = -\frac{2 m_e v}{e B_1 r_o} \qquad \ldots (59)$$

Comparing eqs (57) and (58) with eqs. (43) and (44), we can see that the features of UBS for electrons are the same as for ions except for the sign of Υ. Therefore, it is only necessary to substitute $|\delta_e|$ and $-\Upsilon$ for δ and Υ respectively, and all the discussion in this section is applicable to electrons. Since the direction of gyration is opposite to that for ions, the sign of $\bar{v}_\varphi$ is opposite to that for ions. As a result of the difference in mass, $|\delta_e|$ is much smaller than that for ions of a given particle energy. Therefore, electron motion generally belongs to category (a). Only very high energy electrons can have category (b) motion.

Let W be the particle energy measured in electron volts. Then δ is given by

$$\delta = \pm \frac{2}{r_o B_1} \sqrt{\frac{2m}{e} W} , \qquad \ldots (60)$$

where, the positive sign denotes ions and the negative sign electrons.

4. PARTICLE LOSS

Now, let us investigate the characteristics of particles which will be confined in this toroidal magnetic field. We draw a particle loss diagram having parameters s, Υ and δ. For ions the condition of the confinement is given by

$$|r(\Upsilon_o = 1)|_{max} < r_o . \qquad \ldots (61)$$

(For electrons, $\Upsilon_o = -1$ must be substituted for $\Upsilon_o = 1$). Let us confine the discussion to ions. When $4(\delta - 2\mu) > w_1$, $r(\Upsilon_o = 1)$ takes its maximum value for $\theta = o$. When $4(\delta - 2\mu) < w_1$, $r(\Upsilon_o = 1)$ takes the maximum value for $\theta \approx \pi$. Let δ_L be the value of δ which makes

$$4\delta - 2\mu = w_1 . \qquad \ldots (62)$$

Then

$$\delta_L = \frac{Q_1 s^2 + \mu(\eta_1^2 + 7)}{3 + \eta_1 \Upsilon} \qquad \ldots (63)$$

Case 1 $\delta > \delta_L$

Neglecting the terms of ε^2 order, the relation (61) becomes

$$\delta < \delta_s = (1 - s) \frac{(1 + s) + \frac{\varepsilon}{4}(s^2 + 8\mu)}{(1 + \frac{3}{4}\varepsilon) - \Upsilon\{1 + \varepsilon(s - \frac{1}{4})\}} \qquad \ldots (64)$$

If Υ is not too close to unity, δ_s is a decreasing function of s. This means that the closer the initial position is to the limiting surface the worse for confinement. However, if Υ becomes very close to unity, δ_s becomes an increasing function of s. For instance, putting $\Upsilon = 1$, then

$$\delta < \delta_s = \frac{1}{\varepsilon}\left\{(1+s) + \frac{\varepsilon}{4}(s^2+8\mu)\right\} \qquad \cdots (65)$$

Therefore, when $\Upsilon = 1$, the closer the initial position is to the limiting surface, the higher the energy of the particles confined. This may seem strange, but the reason is as follows. Referring to Fig.6, consider a change of particle orbit caused by changing the particle energy, namely δ, for a fixed initial position, s. For low energy, the orbit is given by the curve a. As the energy is increased, the orbit changes to the curve b' and then to the curve b. Further increase of energy provides the orbit given by Fig.8, where the initial position is P_1. In this case, UBS is given by Fig.7. By increasing the energy further P_2 in Fig.7 approaches P_1 and the UBS degenerates finally to the point P_1; the orbit becomes a circle. In Fig.15, UBS changes from a, b to the point A_1 as the energy increases. By increasing the energy further, UBS becomes UBS(c). The initial position is on the edge of UBS closest to the minor axis. Since UBS(c) makes contact with the limiting surface, $r = r_o$, δ of UBS(c) gives the highest allowable energy for confinement, i.e. δ_s in eq. (65). By moving A_1 toward A_4 the cross section of UBS becomes smaller and finally degenerates to A_4 providing larger δ_s. Therefore, δ_s is an increasing function of s for the case when $\Upsilon = 1$.

Putting $s = 1$ in eq. (65) yields

$$\delta_s \approx \frac{2}{\varepsilon}\left(1 + \frac{\varepsilon}{8} + \mu\right). \qquad \cdots (66)$$

This is the maximum allowable energy in this system. We can obtain this value from other considerations. Since the particle orbit is a circle having the radius $R\eta_1$ around the major axis, $R\eta_1$ should satisfy the following condition;

$$R\eta_1 = \frac{v}{\frac{q}{m}(B_\theta + B_v)} \quad \text{for } s = 1,\ \theta = o. \qquad \cdots (67)$$

Referring to eqs. (11), (21) and (40), eq. (67) yields

$$\delta = \frac{2}{\varepsilon}\left(1 + \frac{3}{8}\varepsilon + \mu\right). \qquad \cdots (68)$$

Although eqs (66) and (68) do not agree with each other, since the approximation of eq. (64) becomes worse for Υ close to unity, the difference is only the factor of $\varepsilon/4$. We can say that the agreement between eqs.(66) and (68) is fairly good.

Case 2 $\delta < \delta_L$

The relation (61) becomes

$$\delta < \delta_S = (1+s)\,\frac{(1-s) - \frac{\varepsilon}{4}\,(s^2+8\mu)}{(1-\frac{3}{4}\varepsilon) - \Upsilon\{1+\varepsilon(s+\frac{1}{4})\}} \,. \qquad \ldots (69)$$

As Υ approaches to $(1-\frac{3}{4}\varepsilon)/\{1+\varepsilon(s+\frac{1}{4})\}$, δ_S becomes very large. However, δ should be limited by the relation $\delta < \delta_L$. For $\delta > \delta_L$ we should use eq. (64).

Let $\varepsilon = 0.05$ and $\mu = 0.66$. From eqs (60), (64) and (69) we can draw the diagram of the maximum allowable δ for confinement for given s and Υ as shown in Figs. 16 and 17.

From Figs.16 and 17, we can conclude that the confinement of duterium ions has a strong dependence on Υ and s, especially for Υ. $\Upsilon = 1$ always provides the maximum δ (i.e., the maximum particle energy) for confinement. As Υ decreases from unity, the maximum δ rapidly drops to a lower value. It shows also a strong asymmetry with erespect to the sign of Υ. For the initial condition that $\Upsilon < o$, only very low δ ions are confined. Although the allowable maximum δ for high Υ ions is high, as soon as the ion changes its Υ value by collision and its δ,Υ,s values drops to the upper region of the curve, the ion will be lost. Only by increasing B_1, can we supress the loss rate.

For electrons, UBS is given by eqs. (57) and (58). Therefore, all the discussion in this section is applicable for electrons simply by substituting $|\delta_e|$ and $-\Upsilon$ for δ and Υ, respectively. Then, the δ, Υ, s diagram in Figs 16 and 17 is applicable for electrons by multiplying the Υ-coordinate by the factor -1.

Since δ is inversely proportional to B_1, the particle confinement is rapidly improved by increasing B_1. Since $m_e << m_i$, the confinement for electrons is much better than for ions, for a given energy. For very high energy electrons, the probability of collision will be greatly decreased. Therefore electrons having such a high energy and Υ close to -1 will be well confined in this system.

For duterium, ions having $\delta = 31$ are confined when $\Upsilon = 1$ and $s = 0.5$. However, the allowable maximum δ is only 0.67 when $\Upsilon = o$ and $s = 0.5$, and 0.32 when $\Upsilon = -1$ and $s = 0.5$. Since most high energy ions have category (b) motion and $\bar{v}_\varphi$ is positive for them, this strong asymmetry for confinement with respect to Υ will result in an axial current in the positive $-\varphi$ direction. Taking into account the electron confinement emphasizes this conclusion.

The result of using the kinetic energy in electron volts, instead of δ, is shown in Figs. 18 and 19, assuming that $B_1 = 1.46 \times 10^{-2}$ Web.m^{-2} and $r_o = 5$ cm.

5. THE CHARGED PARTICLE MOTION IN A TOROIDAL MAGNETIC FIELD WITH ROTATIONAL TRANSFORM AND ELECTRIC FIELD

In the preceeding sections, we discussed the charged particle motion in a toroidal magnetic field disregarding the electric fields which are always present and which have a strong effect on particle confinement. Here, we consider two kinds of electric field. One is the electric field produced by the vertical charge separation due to the U-bend drift. The other is the electric field produced by the radial charge separation due to the difference of confinement between ions and electrons as described in the preceeding section.

Assume the electric charge density distribution is given by

$$\rho^* = \rho_1^* + \rho_2^* \quad , \qquad \ldots (70)$$

where

$$\rho_1^* = - \frac{m_i n_o}{B_o^2} \frac{2E_1 r}{r_o^2 \eta} (2 - \eta) \sin\theta \quad ,$$

$$\rho_2^* = - \frac{m_i n_o}{B_o^2} \frac{E_2}{r_o \eta} \left\{ (1+\eta) \left(1 - \frac{r^2}{r_o^2}\right) - \frac{2r^2}{r_o^2} \right\} . \qquad \ldots (71)$$

ρ_1^* is the vertical charge density distribution due to U-bend drift and ρ_2^* the radial charge density distribution due to the radial charge separation. E_1 and E_2 are constants, and n_o is the plasma density on the minor axis. Assume that the plasma density distribution is given by

$$n = n_o \left\{ 1 - \left(\frac{r}{r_o}\right)^2 \right\} . \qquad \ldots (72)$$

The plasma dielectric constant ε^* is given by

$$\varepsilon^* \cong \frac{m_i n_o}{B_\varphi^2} = \eta^2 \frac{m_i n_o}{B_o^2} \quad . \qquad \ldots (73)$$

Here, it is also assumed that $B_\varphi^2 >> B_\theta^2$ or B_r^2. Solving Poisson's equation for the inhomogeneous dielectric medium;

$$\underline{\nabla}^2 \psi = - \frac{\rho^*}{\varepsilon^*} - \frac{1}{\varepsilon^*} (\underline{\nabla} \varepsilon^*) \cdot (\underline{\nabla} \psi) \qquad \ldots (74)$$

we have the scalar potential ψ of the electric field produced by the charge density given by eqs. (70) and (71).

$$\psi = \psi_1 + \psi_2 \quad , \qquad \ldots (75)$$

where,

$$\psi_1 = - E_1 \frac{r \sin\theta}{\eta^2} \quad ,$$

$$\psi_2 = E_2 \frac{r^2}{2r_o\eta^2} \quad . \qquad \ldots (76)$$

The electric field is given by

$$\underline{E} = \underline{e}_r \left\{ - E_2 \frac{r}{r_o\eta^3} - E_1 \frac{\sin\theta}{\eta^2} \left(1 - \frac{2r\cos\theta}{\eta R} \right) \right\}$$

$$+ \underline{e}_o \left\{ - E_2 \frac{r^2}{r_o\eta^3} \frac{\sin\theta}{R} + E_1 \frac{1}{\eta^2} \left(\cos\theta + \frac{2r\sin^2\theta}{R\eta} \right) \right\} . \qquad \ldots (77)$$

ψ_1 and ψ_2 are the electric potential due to ρ_1^* and ρ_2^* respectively.

The Lagrangian of the particle is given by

$$L = \frac{m}{2} \underline{v}^2 + q \underline{v}\cdot\underline{A} - q\psi \quad . \qquad \ldots (78)$$

The canonical angular momenta are given by eq. (27). From eq. (30), P_φ is a constant of motion. The other constant of motion, the Hamiltonian, is given by

$$H = \frac{m}{2} \left\{ \dot{r}^2 + (r\dot{\theta})^2 + (R\eta\dot{\varphi})^2 \right\} + q\psi \quad . \qquad \ldots (79)$$

By using eq. (27), we can write

$$H = \frac{1}{2m} \left\{ (P_r - qA_r)^2 + \frac{1}{r^2} (P_\theta - qrA_\theta)^2 \right\} + U'(r, \theta) \, , \qquad \ldots (80)$$

where

$$U' = \frac{1}{2mR^2\eta^2} (P_\varphi - qR\eta A_\varphi)^2 + q\psi = \frac{m}{2} v_\varphi^2 + q\psi \quad . \qquad \ldots (81)$$

Since U' is the function of position alone, U' behaves as an equivalent potential. The allowable region for the particle confinement is given by

$$U' \leqslant H \qquad \ldots (82)$$

In this case v is no longer the constant of motion. Assume that the initial condition of the particle is given by eq. (38). Then, the Hamiltonian is given by

$$H = \tfrac{1}{2} m v_1^2 + q\psi_o \, , \qquad \ldots (83)$$

where

$$\psi_o = \tfrac{1}{2} \left(\frac{s}{\eta_1} \right)^2 E_2 r_o \, , \qquad \ldots (84)$$

and v_1 is the initial value of $v = \sqrt{v_r^2 + v_0^2 + v_\varphi^2}$. Instead of v in eq.(38), we use v_1. Referring to eqs. (81) and (83), eq. (82) becomes

$$\frac{m}{2} v_\varphi^2 + q\psi \leqslant \tfrac{1}{2} m v_1^2 + q\psi_0 = H \text{ .. const.} \qquad \text{... (85)}$$

Put

$$U' = \frac{m}{2} v_\varphi^2 + q\psi = \Upsilon_0^2 H \ , \qquad \text{... (86)}$$

where $\Upsilon_0^2 \leqslant 1$. This equation gives a surface on which the equivalent potential U' is equal to $\Upsilon_0^2 H$, which is constant. Let

$$\left.\begin{aligned} \Upsilon &= v_{\varphi 1} / \sqrt{\frac{2}{m} H} \quad , \qquad \delta = \frac{2}{\omega_1 r_0} \sqrt{\frac{2}{m} H} \ , \\ K_V &= \frac{8}{\omega_1 r_0} \frac{E_1}{B_1} \quad , \qquad K_r = \frac{4}{\omega_1 r_0} \frac{E_2}{B_1} \ . \end{aligned}\right\} \qquad \text{... (87)}$$

Referring to eqs. (9), (13), (15), (21), (75), (76), (81) and (87), we can write eq. (86) as follows

$$\left\{ g + \left(\frac{r}{r_0}\right)^2 Q + \mu\eta^2 \right\}^2 = \Upsilon_0^2 \eta^2 \delta^2 - K_r \left(\frac{r}{r_0}\right)^2 + K_V \frac{r}{r_0} \sin\theta$$

$$g = \eta_1 \Upsilon \delta - s^2 Q_1 - \mu \eta_1^2 \ . \qquad \text{... (88)}$$

When $\Upsilon_0^2 \eta^2 \delta^2$ is larger than the rest of the terms of the right hand side of eq. (88), taking the square root of both sides of the inequality and developing the root of the right hand side, finally we have the constant Υ_0 surface, $r = r(\Upsilon_0)$. UBS is given by $r = r(\Upsilon_0 = 1)$, and LBS by $r = r(\Upsilon_0 = -1)$.

$$\begin{aligned} r(\Upsilon_0 = 1) = r_0 \Bigg[& 1 + \frac{\varepsilon^2}{32} w_1 + \frac{\varepsilon^2}{4} \cos^2\theta \left(\delta + 2\mu - \tfrac{3}{4} w_1\right) \\ & + \frac{1}{2\delta} \left\{ K_r + \frac{\varepsilon}{8} K_V \sin\theta \left(5 + \frac{K_V}{\delta^2} \sin\theta \right) \right\} \Bigg]^{-1} \\ & \times \Bigg(\Bigg[w_1 + \frac{\varepsilon^2}{32} w_1^2 + \frac{\varepsilon^2}{4} \cos^2\theta \left\{ (\delta - 2\mu)^2 + w_1 \left(\frac{\delta}{2} - \frac{11}{16} w_1 + 3\mu \right) \right\} \\ & + \frac{K_r}{2\delta} w_1 + \frac{\varepsilon}{16} \frac{K_V}{\delta} \sin 2\theta \left\{ \frac{9}{2} w_1 + 2(\delta - 2\mu) \right\} \\ & + \frac{1}{16} \frac{K_V^2}{\delta^2} \sin^2\theta \left(1 + 2\varepsilon \frac{w_1}{\delta^2} \cos\theta \right) \Bigg]^{\frac{1}{2}} \\ & + \frac{\varepsilon}{8} \cos\theta \left\{ 4(\delta - 2\mu) - w_1 \right\} + \frac{K_V}{4\delta} \sin\theta \Bigg) \ , \end{aligned} \qquad \text{... (89)}$$

where

$$w_1 = s^2 Q_1 + \mu(\eta_1^2 - 1) + \delta(1 - \eta_1 \Upsilon) \qquad \text{... (90)}$$

It is clear that referring to eqs. (27), (80) and (86), we have $v_r^2 + v_\theta^2 = 0$ for $\gamma_0^2 = 1$. Therefore, as mentioned in the preceeding section, the particle motion is limited inside the UBS or between the UBS and LBS. By putting $K_r = K_v = 0$, eq.(89) naturally reduces to eq. (41). As δ increases, the terms in K_r and K_v become small. Therefore, for high energy particles, the effect of the electric field is small. However, for low energy particles, the effect is large.

If K_r is sufficiently large compared with the other parameters, we can satisfy the relation (85) for arbitrary large δ and for $r < r_0$. Thus, K_r is favourable for particle confinement. This result may be an answer to one of the problems mentioned in reference (9). On the other hand, K_v is unfavourable for confinement. Multiplying B_1^2 on both sides of the inequality (88), and putting $B_1 = B_v = 0$, (88) reduces to

$$\eta_1^2 \gamma^2 (\delta B_1)^2 \leqslant \gamma_0^2 \eta^2 (\delta B_1)^2 - K_r B_1^2 \left(\frac{r}{r_0}\right)^2 + K_v B_1^2 \frac{r}{r_0} \sin\theta \qquad \ldots (91)$$

where, δB_1, $K_r B_1^2$ and $K_v B_1^2$ are independent of B_1. From eq.(91), we have the same result as mentioned above. Thus, even without the azimuthal and the vertical magnetic field, ions can be confined by establishing a sufficiently large radial electric field if such a field can be provided.

To get some idea of the effect of an electric field, neglecting small terms, the UBS can be written approximately,

$$r(\gamma_0 = 1) \approx \frac{r_0}{1 + \frac{K_r}{2\delta}} \left[\left\{ w_1 + \frac{\varepsilon^2}{4} \cos^2\theta \, (\delta - 2\mu)^2 + \frac{K_r}{2\delta} w_1 + \frac{1}{16} \left(\frac{K_v}{\delta}\right)^2 \sin^2\theta \right\}^{1/2} + \frac{\varepsilon}{8} \cos\theta \left\{ 4 (\delta - 2\mu) - w_1 \right\} + \frac{K_v}{4\delta} \sin\theta \right] \qquad \ldots (92)$$

From this equation, we can see easily that larger K_r makes confinement better and that larger K_v results in worse confinement.

From eqs. (83) and (84), we can write

$$H = e \left\{ W \pm \frac{1}{2} \left(\frac{s}{\eta_1}\right)^2 r_0 E_2 \right\} , \qquad \ldots (93)$$

where W is the initial particle kinetic energy in electron volts, and the positive sign corresponds to ions and the negative to electrons. Then we have

$$\left.\begin{aligned} \frac{K_r}{\delta} &= 2\,\frac{E_2}{B_1}\,\sqrt{\frac{2e}{m}\left\{W \pm \frac{1}{2}\left(\frac{s}{\eta_1}\right)^2 r_o\,E_2\right\}}\,, \\ \frac{K_v}{\delta} &= 4\,\frac{E_1}{B_1}\,\sqrt{\frac{2e}{m}\left\{W \pm \frac{1}{2}\left(\frac{s}{\eta_1}\right)^2 r_o\,E_2\right\}}\,. \end{aligned}\right\} \qquad \cdots (94)$$

The condition of the particle confinement is obtained by

$$r(\Upsilon_o = 1)_{max} < r_o \qquad \cdots (95)$$

For example, let $E_1 = 75.1$ V m^{-1}, $E_2 = 200$ V m^{-1}, $B_1 = 1.46 \times 10^{-2}$ Wb m^{-2}, $B_V = 4.81 \times 10^{-4}$ Wb m^{-2}, $r_o = 5 \times 10^{-2}$m and $R = 1$m. Then the maximum permissible kinetic energy for confinement for given s and Υ similar to Fig.18 and 19 is shown in Fig.20 and 21 for duterium ions.

For particles having small δ, we cannot use eq. (89) since the expansion (88) is impossible. In this case, we have to use (88) as it is, or we can use the relation

$$0 \leqslant \eta^2\,\delta^2 - K_r\left(\frac{r}{r_o}\right)^2 + K_V\,\frac{r}{r_o}\sin\theta\,. \qquad \cdots (96)$$

Since the magnetic field has no effect on the particle kinetic energy, the latter is restricted only by the scalar potential of the electric field. Equation (96) gives the restriction. Solving this equation yields

$$r(\Upsilon_o = 1) \leqslant \frac{r_o}{2(K_r - \varepsilon^2\cos^2\theta\,\delta^2)} \qquad \cdots (97)$$

$$\times\left\{K_V\sin\theta + 2\,\varepsilon\cos\theta\,\delta^2 + \sqrt{K_V\sin\theta\,(K_V\sin\theta + 4\,\varepsilon\cos\theta\,\delta^2) + 4\,\delta^2 K_r}\right\}.$$

As seen already in eq. (89), $r = r(\Upsilon_o = 1)$ surface shifts in the region, $\sin\theta > o$, namely towards the negative z direction. This shift is due to K_V, namely the vertical electric field, which makes the confinement worse. Only the effect of K_r, the radial electric field, can suppress the effect of K_V. Of course, the stronger the magnetic field, the smaller K_r and K_V become, thus eliminating the effect of electric fields.

6. TRAPPED PARTICLES BY THE MIRROR EFFECT

In the preceeding discussion, we have not used the adiabatic invariant. However, if we consider the adiabatic invariant, for example $\mu^* = \frac{1}{2} mv_\perp^2 / B$, the particles will be influenced by the mirror effect as they move in the magnetic field. Then, the longitudinal field B_a becomes significant. The particles motion will be limited to the region

$$- \theta_m \leqslant \theta \leqslant \theta_m \ , \qquad \ldots (98)$$

as shown in Fig.22. First we consider the case without electric fields. When $\delta > \delta_L$ (high energy particles) the maximum value of $r = r(\Upsilon_o = 1)$ occurs when $\theta = 0$. Therefore, the additional restriction on the motion given by eq.(98) makes no change to the particle confinement.

However, when $\delta < \delta_L$ (very low energy particles) the maximum value of $r = r(\Upsilon_o = 1)$ occurs when $\theta = \pi$ as shown in Fig.23. In this case, the particle suffers the mirror effect restriction, $-\theta_m \leqslant \theta \leqslant \theta_m$, and can be confined even if $r(\Upsilon_o = 1)_{max} > r_o$, if $r(\Upsilon_o = 1 \ , \ \theta = o) < r_o$. Therefore, the mirror effect improves the confinement for very low energy particles.

For the case with electric fields, the UBS deforms in the direction of negative z by the effect of $K_v \sin\theta$. Then, if $r(\Upsilon_o = 1 \ , \ \theta = o) < o$, the mirror effect can improve the confinement even if $r(\Upsilon_o = 1)_{max} > r_o$. However, this applies to low energy particles only, since for high energy particles the effect of the electric field becomes small. Note that the calculation in this paper is based on the assumption that $\frac{\partial}{\partial \varphi} \equiv 0$. If $\frac{\partial}{\partial \varphi} \neq 0$, there will be more particles confined by the mirror effect.

7. GUIDING CENTRE LIMIT MODEL

In Section 5, we discussed the particle confinement in the Tokomak type magnetic field and obtained curves for the maximum permitted energy of the particle as a function of the initial position $s = r_1/r_o$ and the initial velocity $\Upsilon = v_{\varphi_1}/v$. The maximum allowable energy W is a monotonically increasing function of Υ and shows a strong asymmetry with respect to the sign of Υ.

In our discussion, neither the adiabatic invariant nor the guiding center limit model was used. If we introduce the simplest guiding center limit model, by solving the following approximate equations

$$\left.\begin{aligned} \underline{v}_z &= \underline{e}_z \, v_u = \underline{e}_z \, \frac{m}{2qB_oR} \left(v_\perp^2 + v_{\parallel}^2\right) \ , \\ \underline{v}_\theta &= \underline{e}_\theta \, r\dot{\theta} = \underline{e}_\theta \, \frac{B_1}{B_o} \, v_{\parallel} \ , \end{aligned}\right\} \qquad \ldots (99)$$

we can plot W against Υ as shown in Fig.24, or $v_\perp$ against $v_\parallel$ as shown in Fig.25. The particle confinement feature is still independent of B_0, the longitudinal field. Fig.25 was obtained by Bishop[10] in his calculation on the particle containment in the Stellarator. This diagram shows on elegant symmetry with respect to the sign of Υ; particles, having the initial condition $v_\parallel = 0$, cannot be confined in this system. However, in our case, such a particle can be confined.

The reason for the discrepancy between Fig.24 and Fig.18 is as follows. Consider a particle whose initial condition is $\theta = 0$, $s = r_1/r_0 < 1$ and $\Upsilon = 0$, namely $v_{\varphi 1} = 0$. The condition, $\Upsilon = 0$, does not mean $v_\parallel = 0$ exactly; however $v_\parallel \approx 0$ if $B_1 \ll B_0$. Or, let $\Upsilon = \Upsilon_s$ which really satisfies the initial condition $v_\parallel = 0$. Whether $\Upsilon = 0$ or $\Upsilon = \Upsilon_s$ makes little difference to the discussion. Let us take two magnetic surfaces of different mean radii, S_1 and S_2 as shown in Fig.26. If the particle is on the magnetic surface S_1, and $v_\parallel = o$, we have $v_\perp^2 = v^2$. The particle moves upward due to the U-bend drift. When the particle arrives at the magnetic surface S_2, since v = const and the pitch of the helical lines of force on S_2 is different from that on S_1, the particle aquires a $v_\parallel$ as shown in Fig.26. Thus the particle starts to move along the helical lines of force and tends to be confined in this system. In the simplest guiding center limit model used by Bishop, he assumed that $v_\parallel$ and $v_\perp$ were constant and equal to the initial values. This is the reason why he obtained a symmetrical picture with respect to the sign of $v_\parallel$, which implies no confinement for $v_\parallel = 0$. If we take into account the mirror effect, the particle having the initial condition $v_\parallel = 0$ can be confined in this guiding center model. An analysis of the adiabatic motion of a particle in a Stellarator field will be found in references (1) and (2).

ACKNOWLEDGMENTS

It is a pleasure to acknowledge valuable discussions on this subject with Dr R.S. Pease, Dr R.J. Bickerton and Dr A. Gibson. This work was performed under the auspices of the United Kingdom Atomic Energy Authority.

REFERENCES

1. MOROZOV, A.I. and SOLOVEV, L.S. The motion of particles in a toroidal crimped magnetic field. Zh. Tekh. Fiz., vol.30, no.3, March, 1960. pp.261-270. (Trans. in Sov. Phys - Tech. Phys., vol.5, no.3, September, 1960. pp.241-249).

2. POPRYADUKHIN, A.P. Pertubations of the particle motion in a stellarator. J. Nucl. Energy Pt.C, vol.8, no.2, March/April, 1966. pp.169-182.

3. HASTIE, R.J., TAYLOR, J.B., and HAAS, F.A. Adiabatic invariants and the equilibrium of magnetically trapped particles. Culham Laboratory, March 1966. CLM-P103

4. TAMM, I.E., Theory of magnetic thermonuclear reactor. Part III. Drift and thermal conductivity of a plasma in a toroid in the presence of a stabilizing current. In LEONTOVICH, M.A., ed. Plasma Physics and the Problem of Controlled thermonuclear reactions. Oxford, Pergamon Press, 1961. vol.1, pp.35-47.

5. LEHNERT, B., On the confinement of charged particles in a magnetic field. J. Nucl. Energy Pt. C, vol.1, nos 1/2, 1959. pp.41-48.

6. SHAFRANOV, V.D., Equilibrium of a toroidal plasma in a magnetic field. J. Nucl. Energy Pt.C, vol.5, no.4, July/August, 1963. pp.251-258.

7. SHAFRANOV, V.D. Equilibrium of a plasma toroid in a magnetic field. Zh. Exper. Teor. Fiz., vol.37, October, 1959. pp.1088-1095. (Trans. in Sov. Phys. - JETP, vol.10, no.4, April, 1960. pp.775-779).

8. ARTSINOVICH, L.A. and KARTASHEV, K.B., Effect of a transverse magnetic field on a toroidal discharge. Dokl. Akad. Nauk, SSSR, vol.146, no.6, October, 1962. pp. 1305-1308. (Trans. in Sov. Phys. - Doklady, vol.7, no.10, April, 1963. pp. 919-921).

9. JANES, G.S. and others., New type of accelerator for heavy ions. Phys. Rev., vol. 145, no.3, 20th May 1966. pp.925-952.

10. BISHOP, A.S. and SMITH, C.G., A microscopic treatment of classical containment in the stellarator. Princeton University, Plasma Physics Laboratory, January 1966. MATT-403.

APPENDIX I

The condition for the vertical field B_V to eliminate the magnetic surface shift due to the dipole-like magnetic field produced by the secondary current is given by

$$B_V \approx \frac{\zeta}{\zeta + 2} \frac{2\pi n_o}{\sigma V_L} k \, (T_{i\perp} + T_{e\perp} + T_{i\parallel} + T_{e\parallel}) \qquad \ldots (A.1)$$

where we assume the plasma density distribution is given by

$$n = n_o \left\{ 1 - \left(\frac{r}{r_o} \right)^{\zeta} \right\} . \qquad \ldots (A.2)$$

ζ is the parameter of the density gradient.

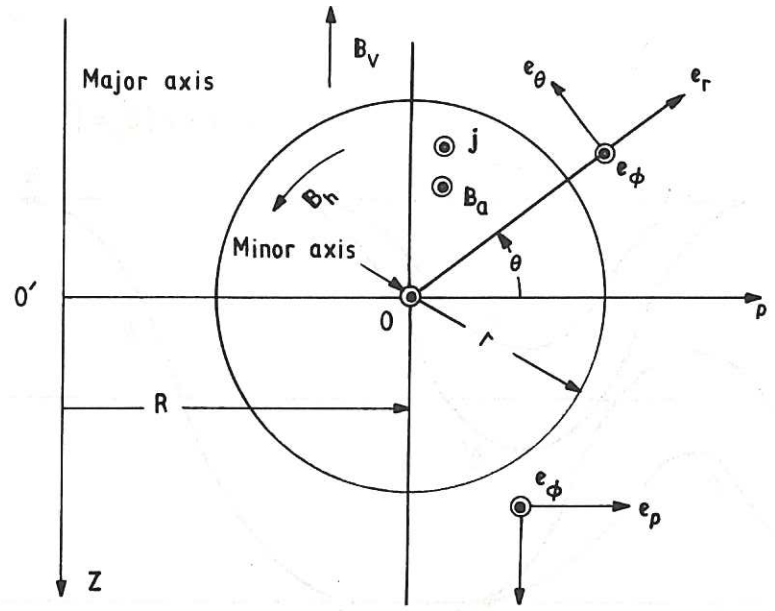

Fig. 1 (CLM-R 67)

Toroidal co-ordinate system (r, θ, ϕ) and cylindrical co-ordinate system (ρ, ϕ, z)

B_a ; longitudinal magnetic field ; B_h ; azimuthal magnetic field

B_V ; vertical magnetic field ; j ; ohmic heating current density

$\odot$; the direction pointing outward from the paper;

ρ ; major radius ; r ; minor radius.

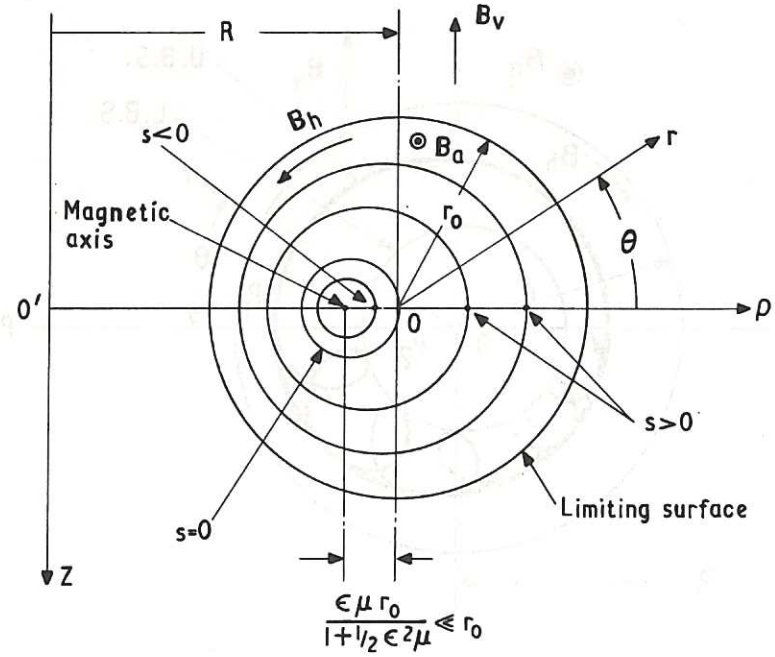

Fig. 2 (CLM-R 67)

Magnetic surfaces and magnetic axis: s is the value of r on the magnetic surface for $\theta = 0$. The position of the magnetic axis is given by

$$(r, \theta) = \left(\frac{\epsilon\,\mu\, r_0}{1+\frac{\epsilon}{2}\,\epsilon^2\,\mu}\,,\ \pi \right) \approx \left(\frac{B_V}{B_t}\, r_0\,,\ \pi \right)$$

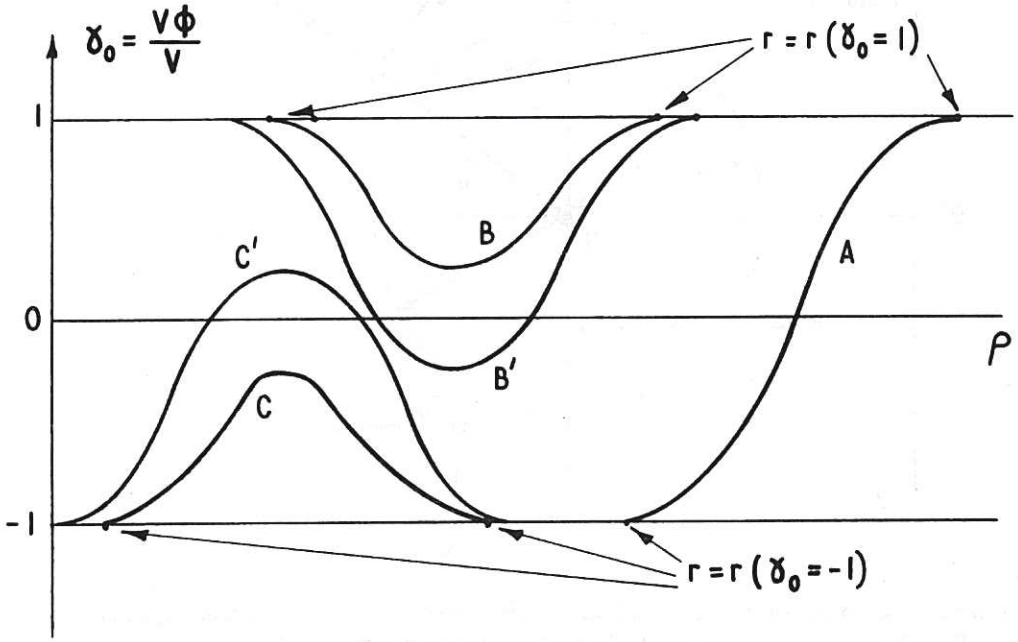

Fig. 3 (CLM-R67)
Allowable range for the particle motion. The motions C and C′ are not permitted for ions. The motions B and B′ are not permitted for electrons

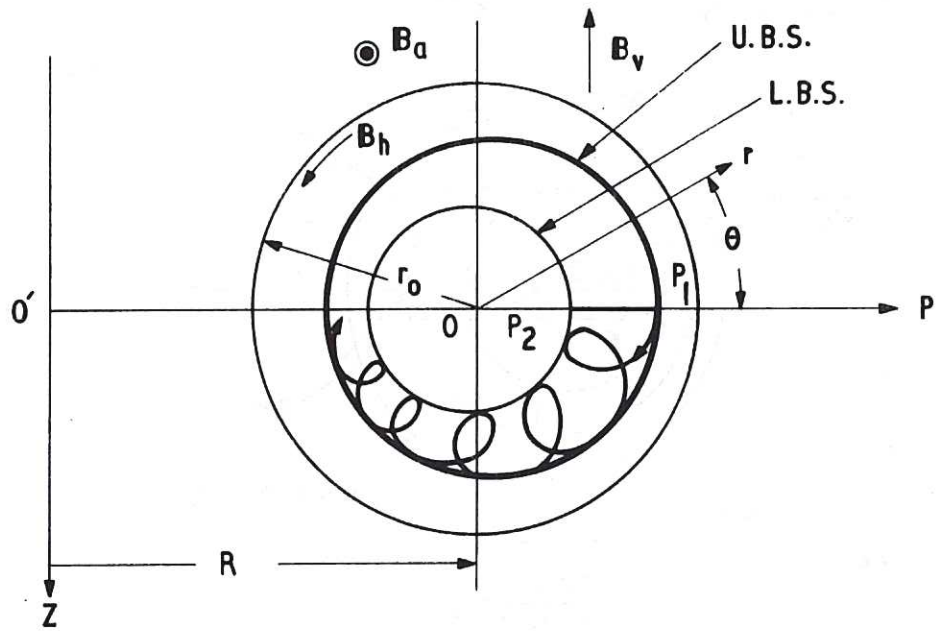

Fig. 4 (CLM-R67)
U B S and L B S of the category (a) motion : $D_1 > 0$, $D_2 > 0$, $s > 0$. The particle motion is restricted in the region between the U B S (upper boundary surface) and the L B S (lower boundary surface)

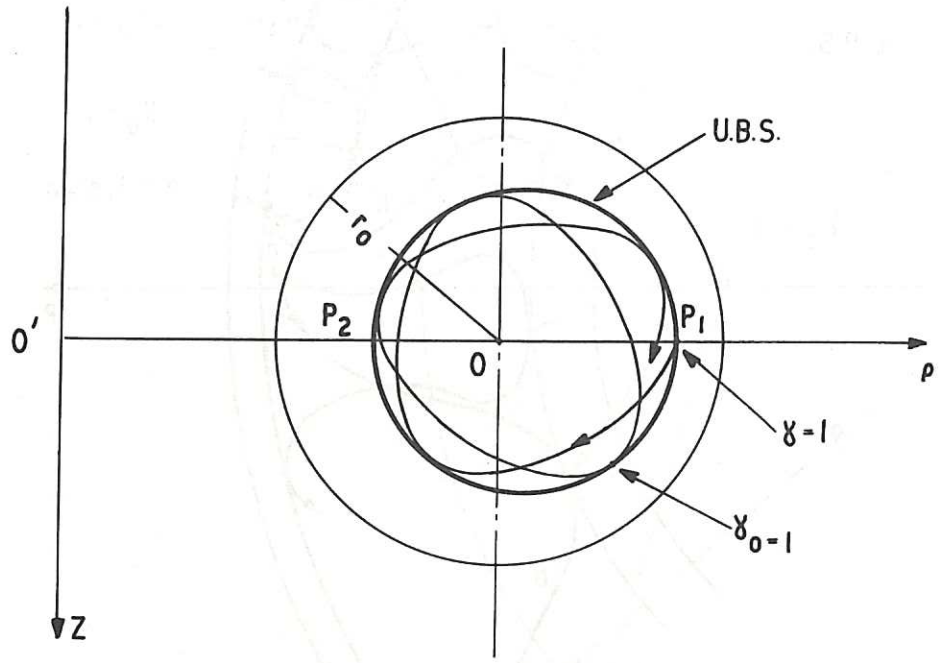

Fig. 5 (CLM-R67)

UBS of category (b) motion: $D_1 > 0$, $D_2 < 0$, $s > 0$, $\gamma = 1$
The particle motion is restricted inside the UBS

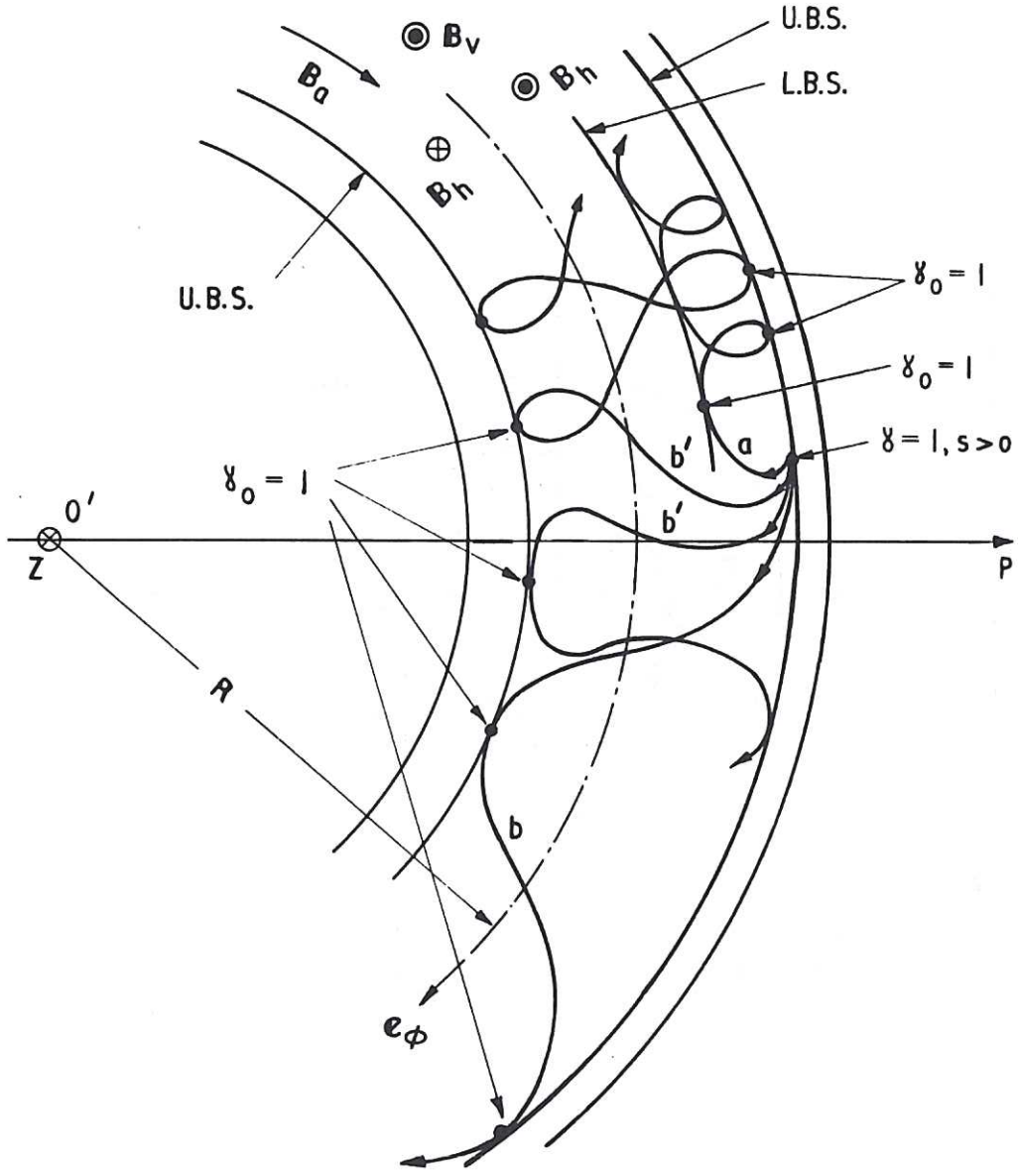

Fig. 6 Particle orbits : $\gamma = 1$, $s > 0$ (CLM-R67)

Curve a ; $-1 \leq \gamma_0 \leq 1$, category (a) motion , small δ

Curve b'; $-1 < \gamma_0 \leq 1$, category B' motion , medium δ

Curve b ; $0 < \gamma_0 \leq 1$, category (b) motion , large δ

$\gamma_0 = \frac{V_\phi}{V}$; instantaneous value of $\frac{V_\phi}{V}$

$\gamma = \frac{V_{\phi 1}}{V}$; initial value of $\frac{V_\phi}{V}$

$\oplus$; the direction pointing inward to the paper

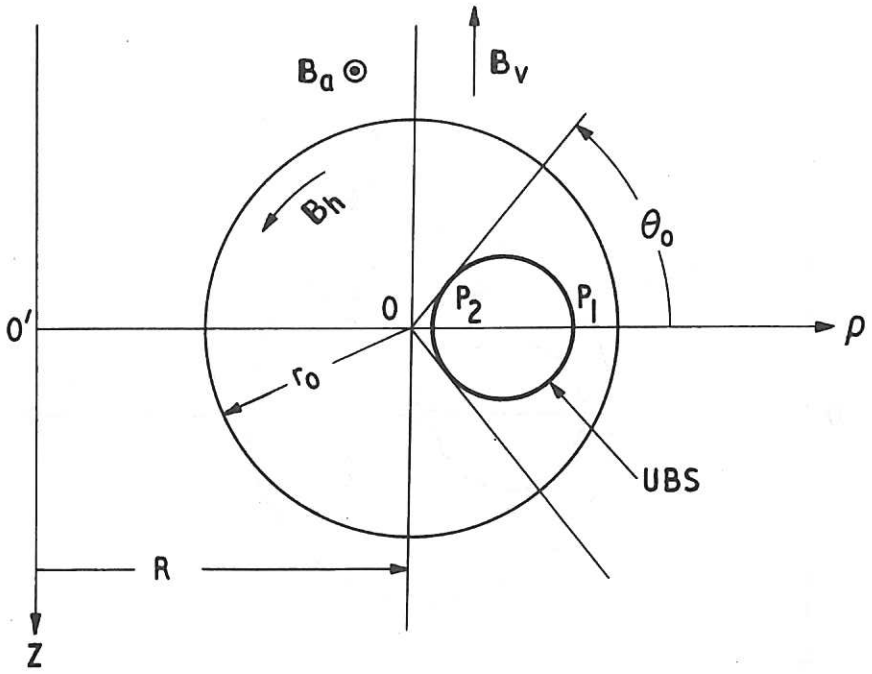

Fig. 7 (CLM-R67)
UBS of the category (b) motion; $D_1 > 0$ for $\cos^2\theta \geq \cos^2\theta_0$; $D_1 < 0$ for $\cos^2\theta < \cos^2\theta_0$; $D_2 < 0$; $\gamma = 1$, $s > 0$

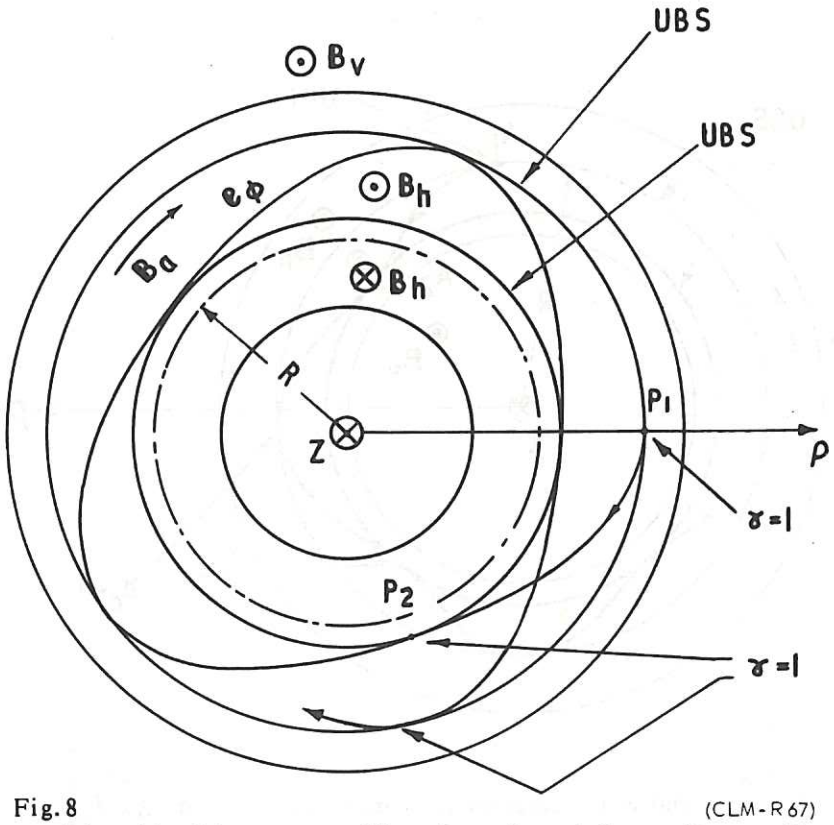

Fig. 8 (CLM-R67)
Particle orbit of the category (b) motion; $D_1 \geq 0$ for $\cos^2\theta \geq \cos^2\theta_0$
$D_1 < 0$ for $\cos^2\theta < \cos^2\theta_0$; $D_2 < 0$; $\gamma = 1$, $s > 0$

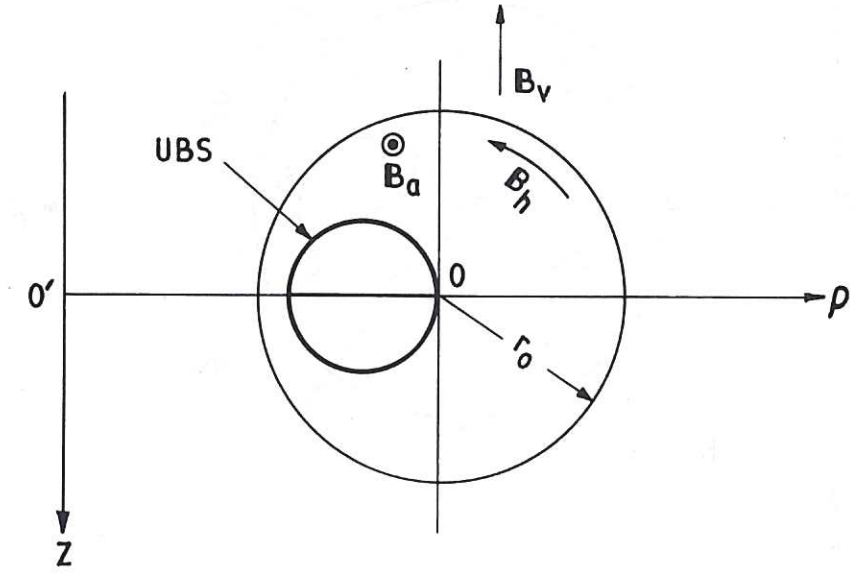

Fig. 9 (CLM-R 67)
UBS of the category (b) motion $\gamma = 1$, $s = 0$, $\delta < 2\mu$

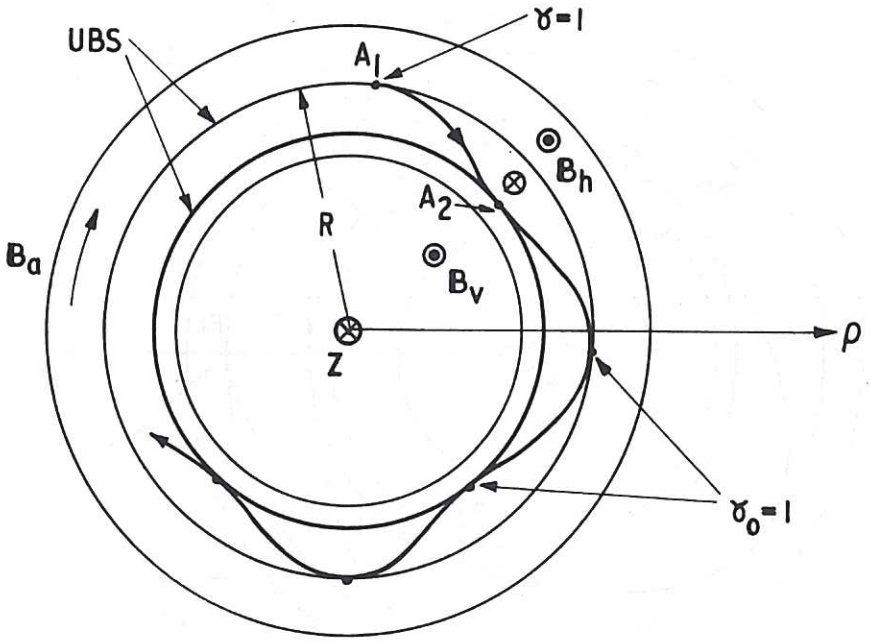

Fig. 10 (CLM-R 67)
Particle orbit of the category (b) motion $\gamma = 1$, $s = 0$, $\delta < 2\mu$

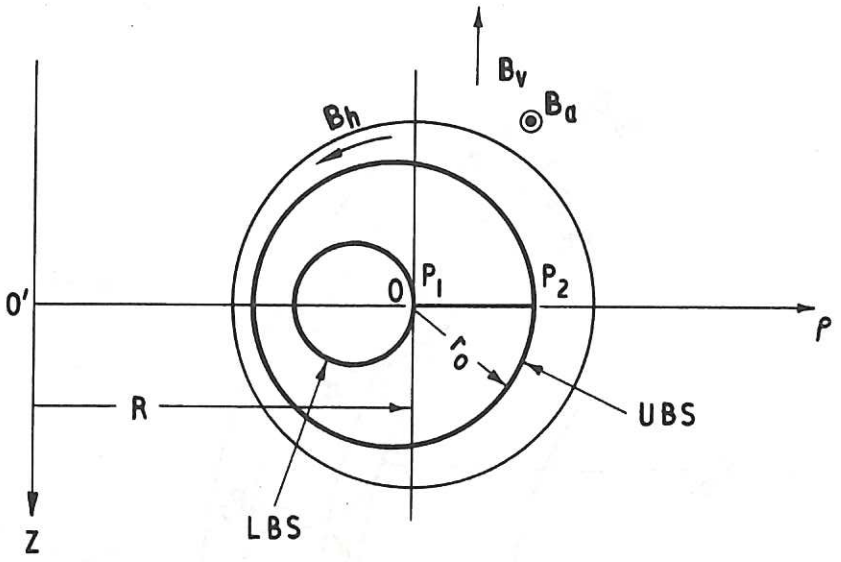

Fig. 11 (CLM-R67)
UBS and LBS of the category (a) motion $\gamma = -1$, $s = 0$

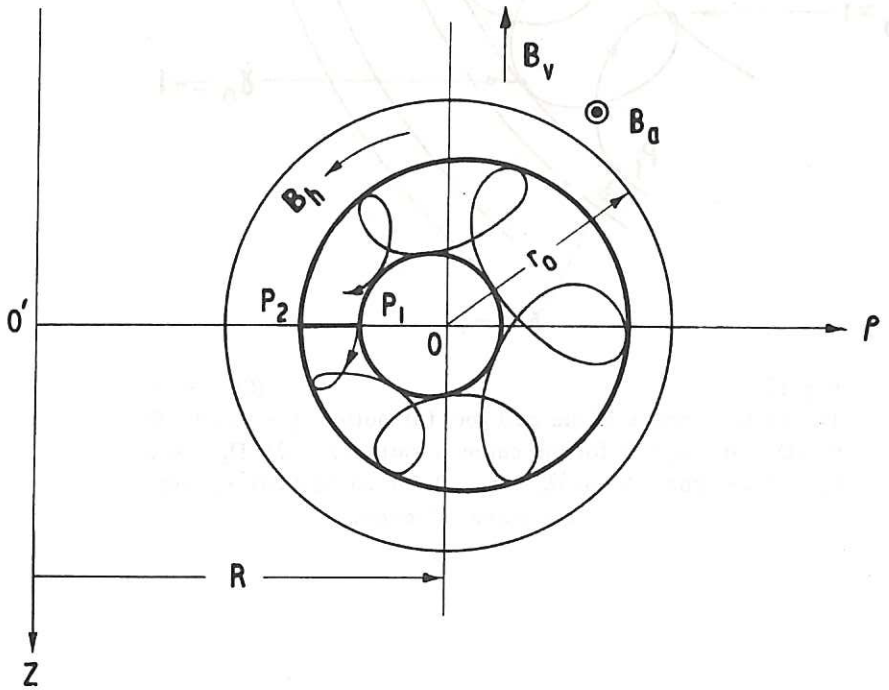

Fig. 12 (CLM-R67)
UBS and LBS of the category (a) motion
$\gamma = -1$, $s < 0$, $D_1 > 0$, $D_2 < 0$

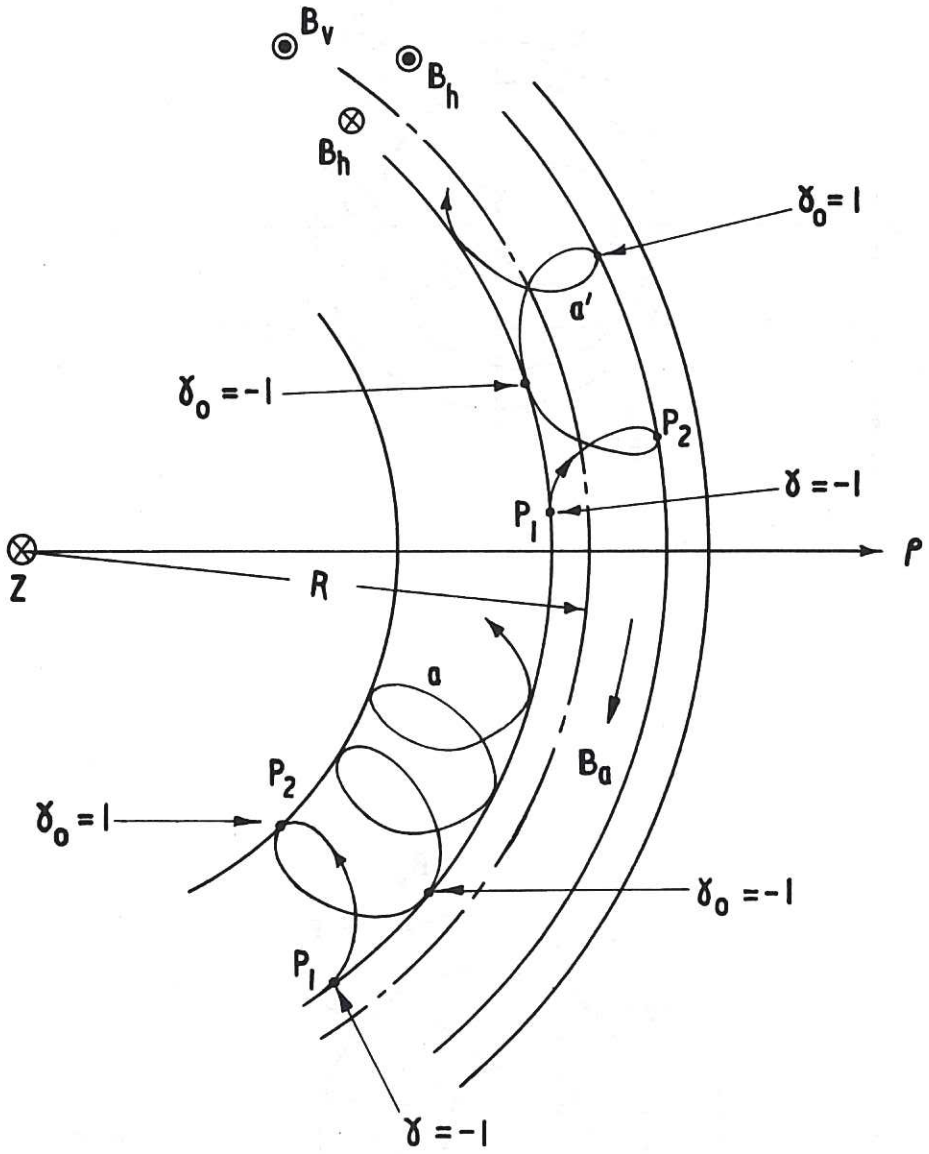

Fig. 13 (CLM-R67)

The particle orbits of the category (a) motion $\gamma = -1$, $s < 0$ (1) $D_1 > 0$, $D_2 > 0$ for the curve a motion; (2) $D_1 > 0$, $D_2 \geq 0$ for $\cos^2\theta \geq \cos^2\theta_0'$; $D_2 < 0$ for $\cos^2\theta < \cos^2\theta_0'$ for the curve a' motion

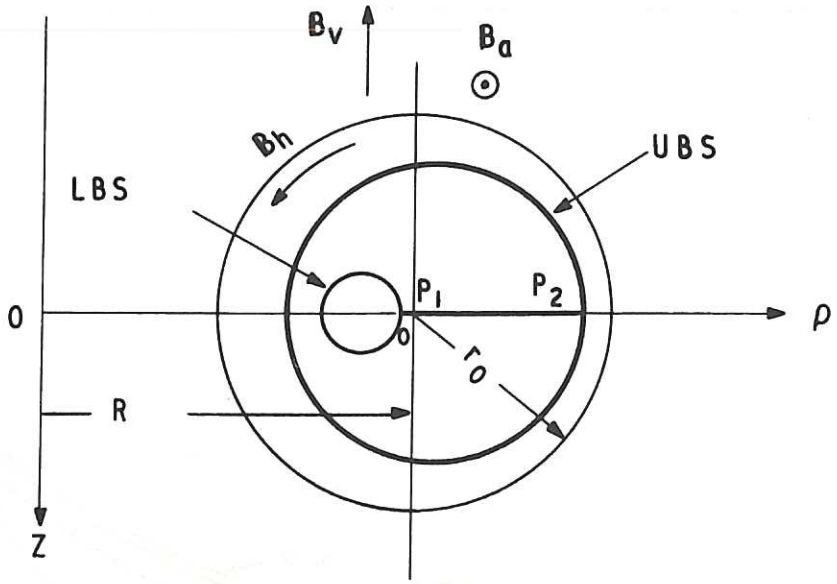

Fig. 14 (CLM-R 67)
UBS and LBS of the category (a) motion $\gamma = 1$, $s < 0$, $D_1 > 0$
$D_2 \geq 0$ for $\cos^2\theta \geq \cos^2\theta_0'$; $D_2 < 0$ for $\cos^2\theta < \cos^2\theta_0'$

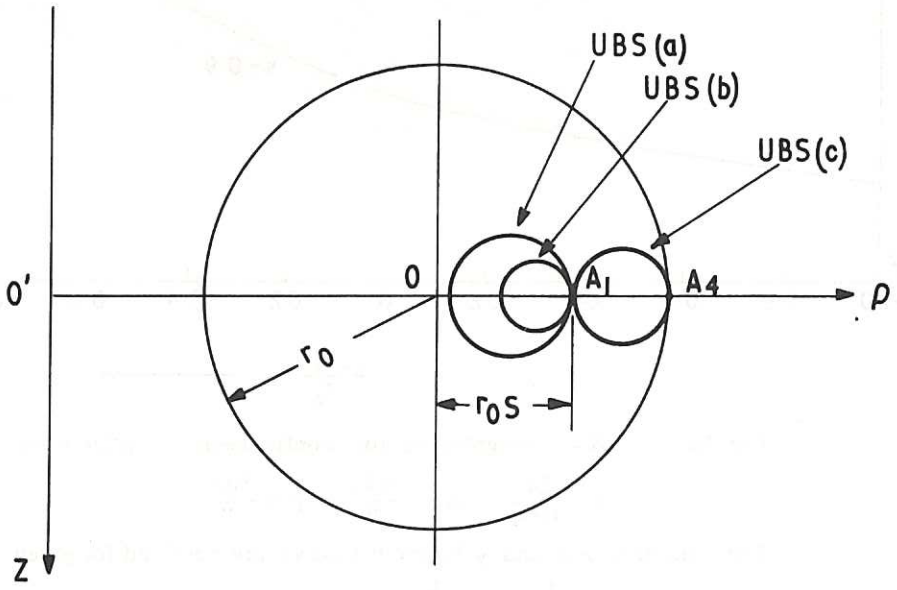

Fig. 15 (CLM-R 67)
UBS for different initial energy with $\gamma = 1$. $\gamma = 1$, $s > 0$,
USB changes from (a) → (b) → (A_1) → (c), as δ increases

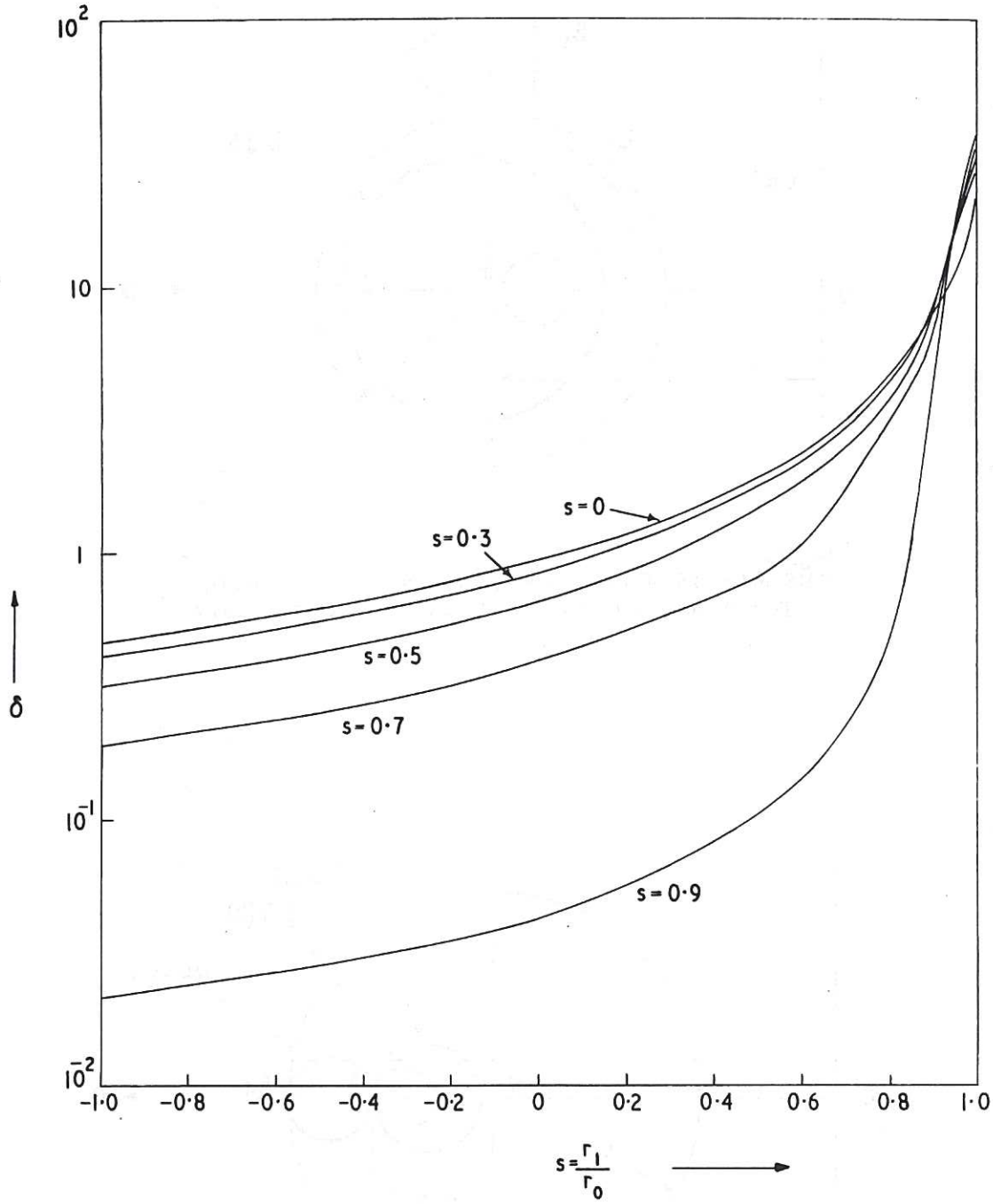

Fig. 16 $\delta - \gamma$ diagram of ion confinement (CLM-R 67)

$$\delta = \frac{2v}{r_0 \omega_1}, \quad \omega_1 = \frac{q B_1}{m}, \quad \gamma = \frac{v_{\phi 1}}{v}$$

The ions having δ and γ below the curve are confined for given

$$s = \frac{r_1}{r_0} \; ; \quad \epsilon = \frac{r_0}{R} = 0.05 \; ; \quad \mu = 0.66$$

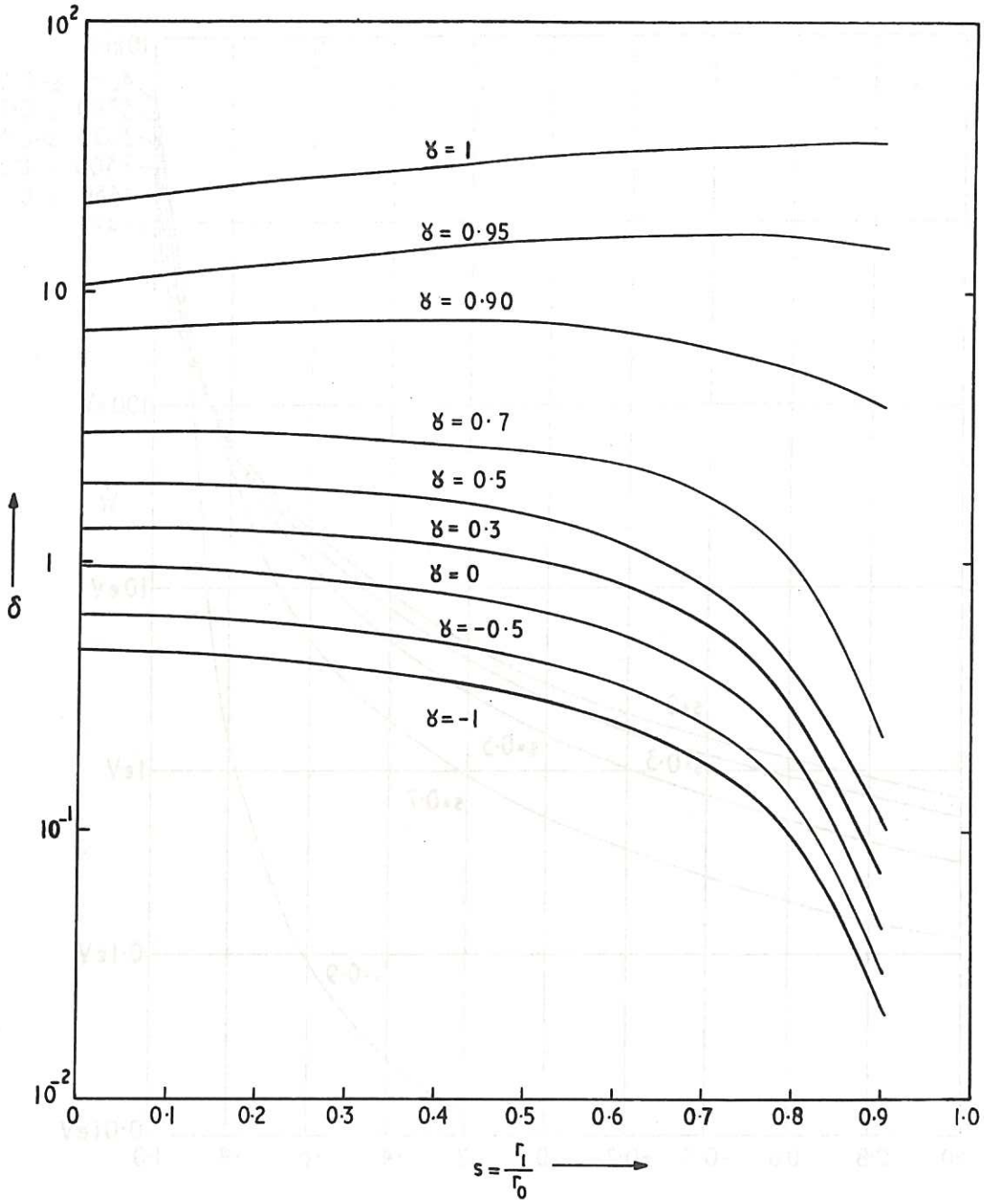

Fig. 17 δ – s diagram of ion confinement (CLM-R67)

$$\delta = \frac{2v}{r_0 \omega_1}, \quad \omega_1 = \frac{q B_1}{m}, \quad \gamma = \frac{v_{\phi 1}}{v}$$

The ions having δ and s below the curve are confined for given γ

$$\epsilon = \frac{r_0}{R} = 0.05, \quad \mu = 0.66$$

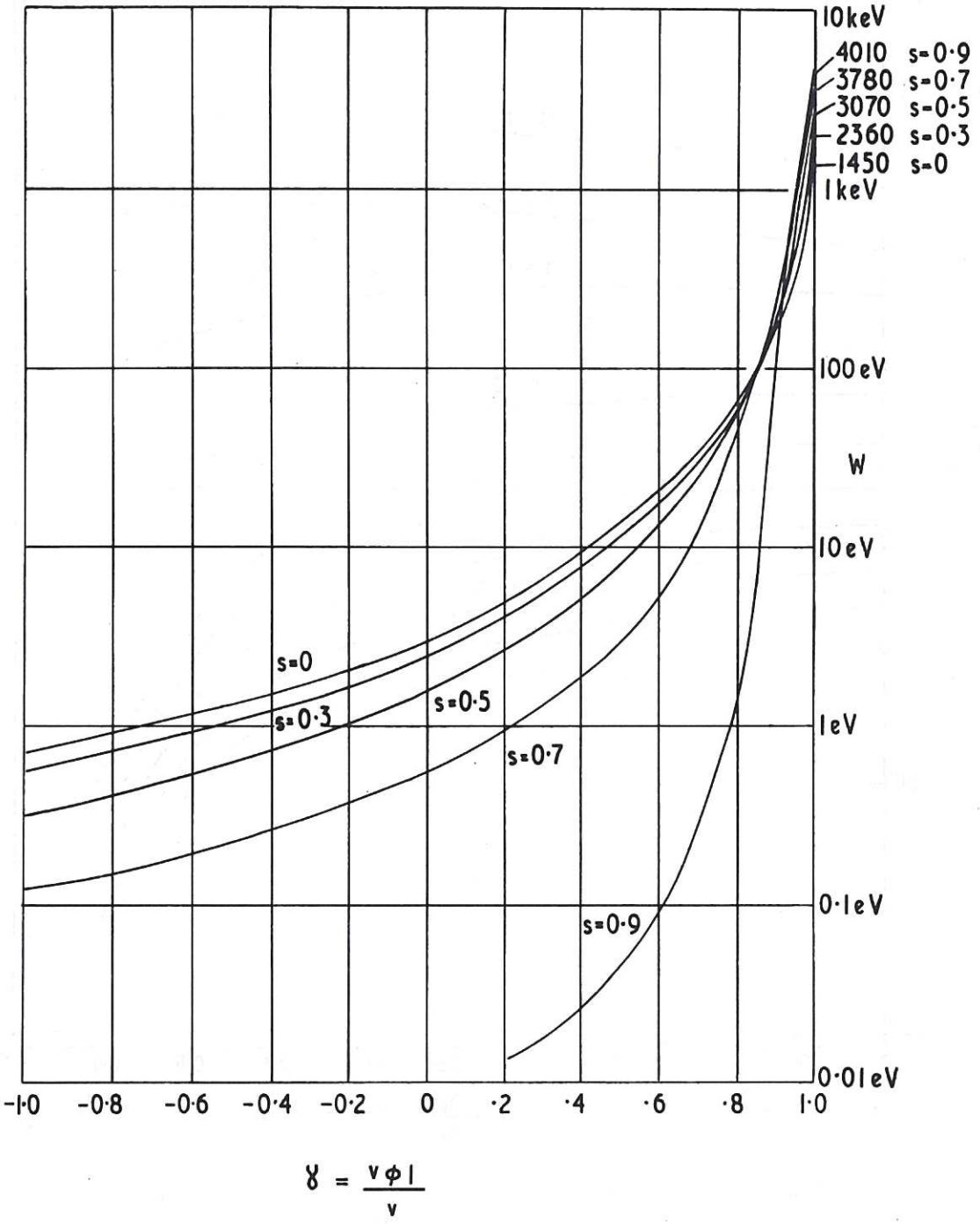

Fig. 18 (CLM-R67)

W - γ diagram of deuterium ion confinement. The ions which have W and γ below the curve are confined

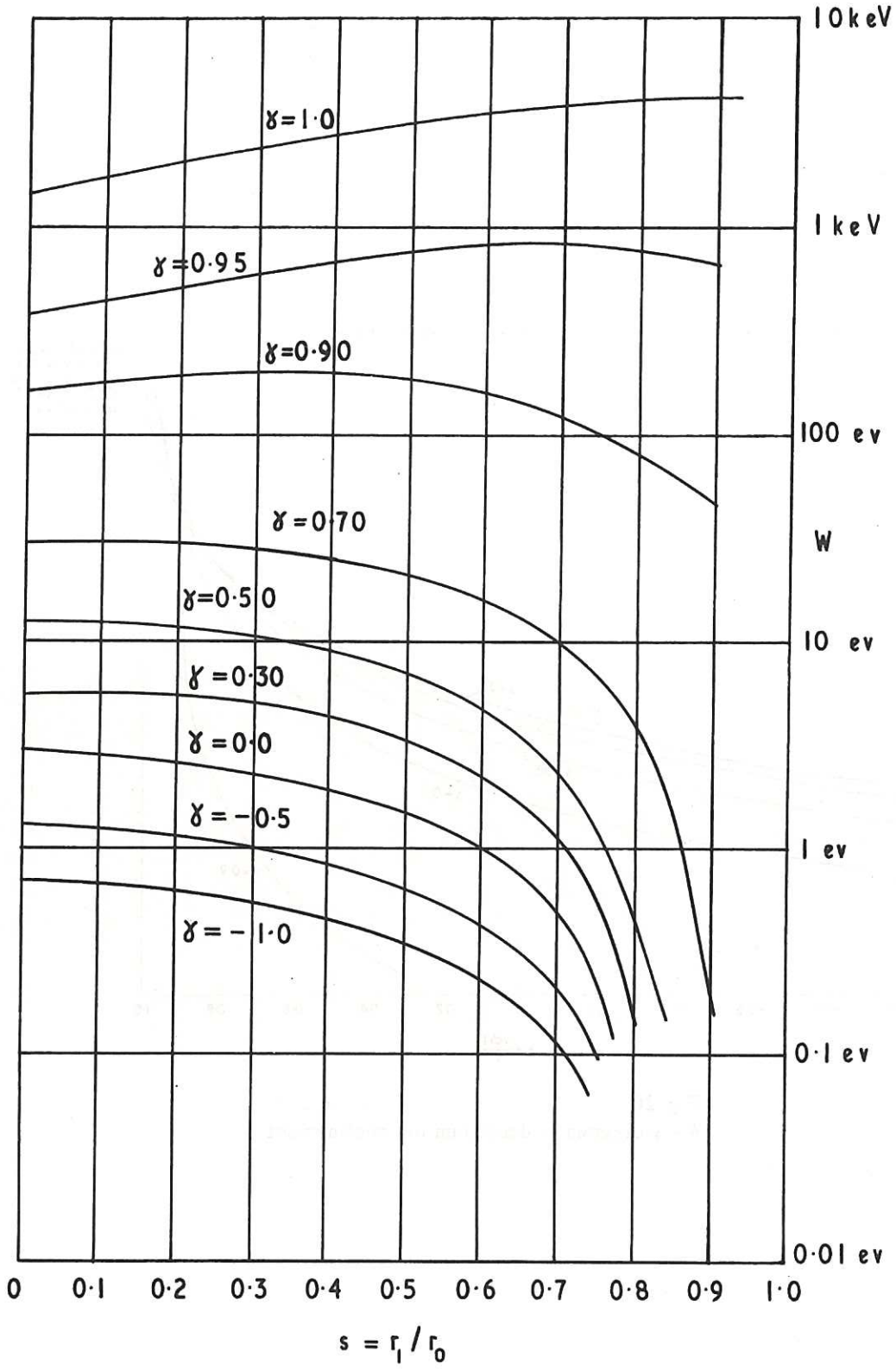

Fig. 19 (CLM-R67)

W - s diagram of the deuterium ion confinement. The ions which have W and s below the curve are confined

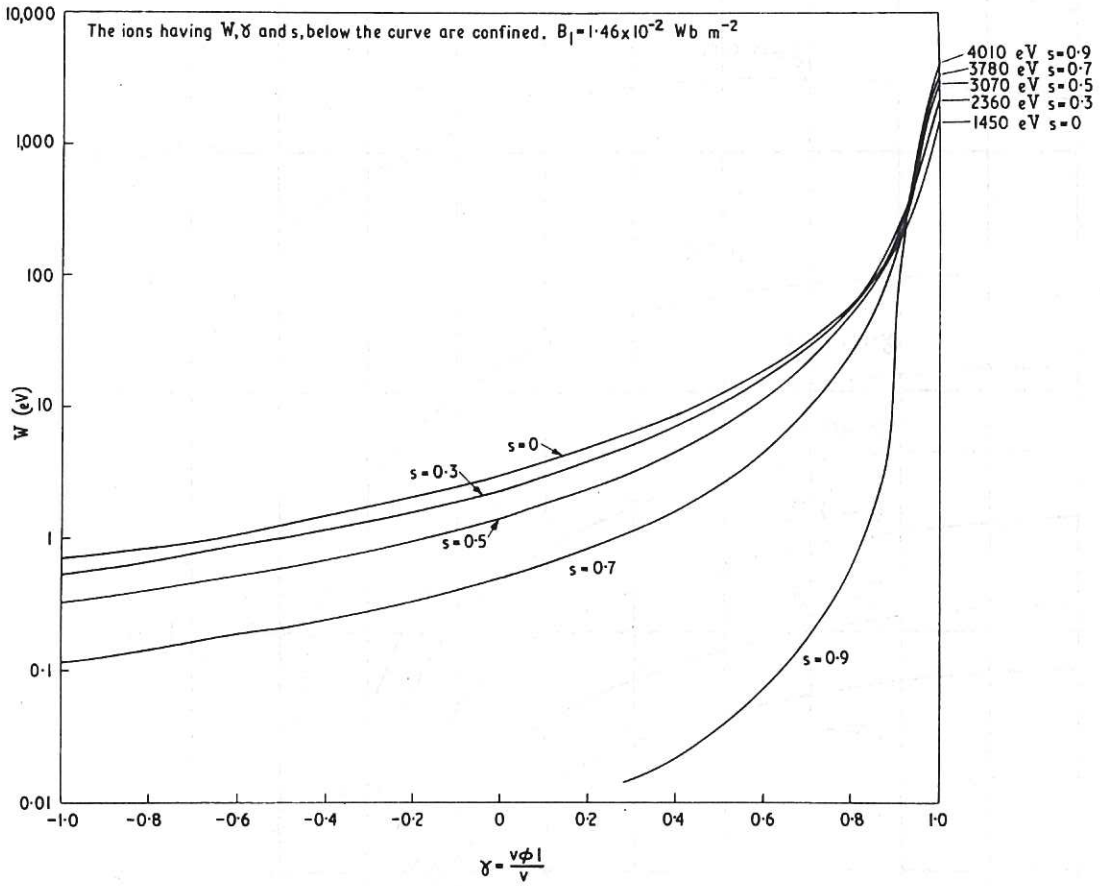

Fig. 20 (CLM-R67)
W - γ diagram of deuterium ion confinement

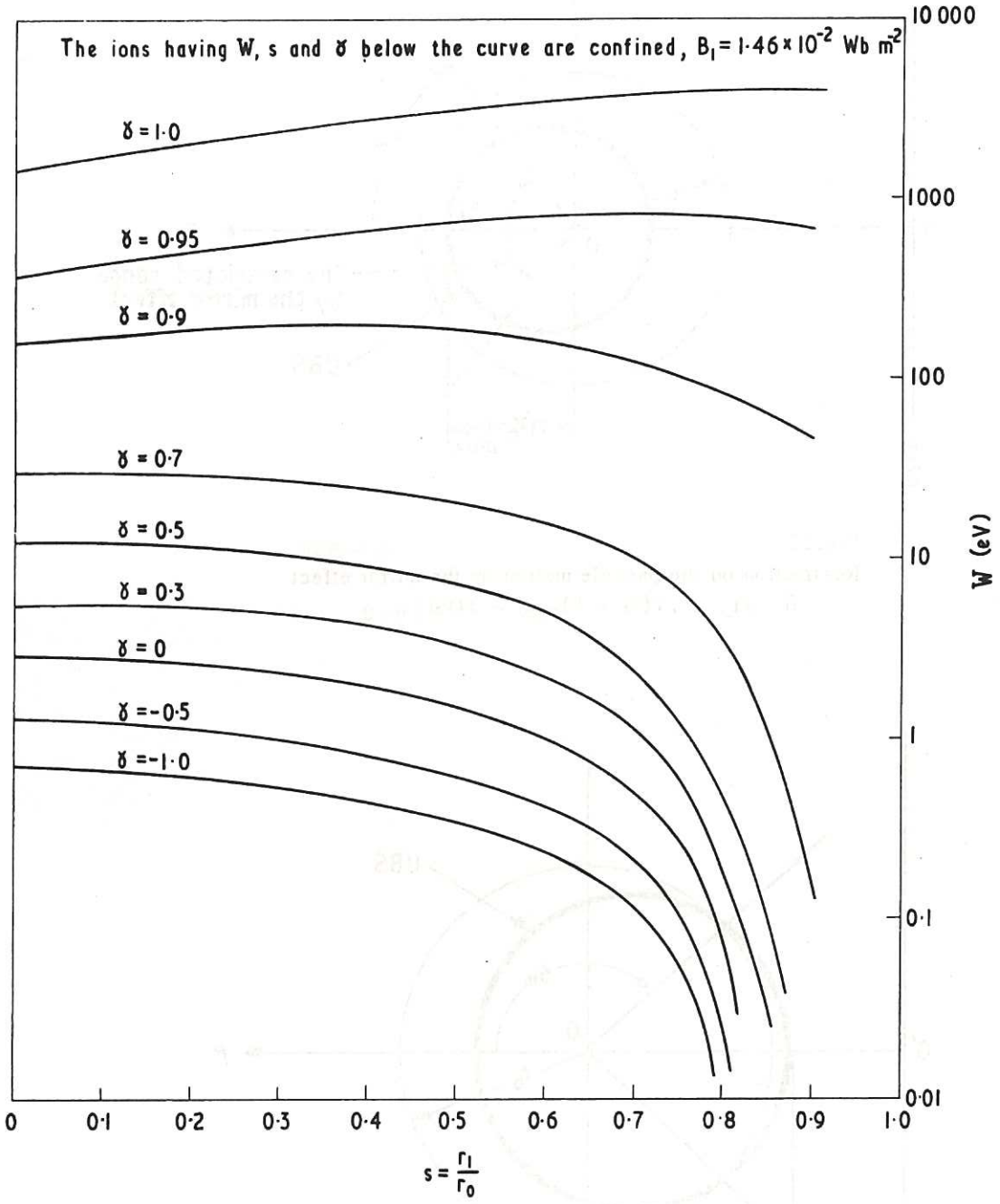

Fig. 21 (CLM-R67)
W - s diagram of deuterium ion confinement

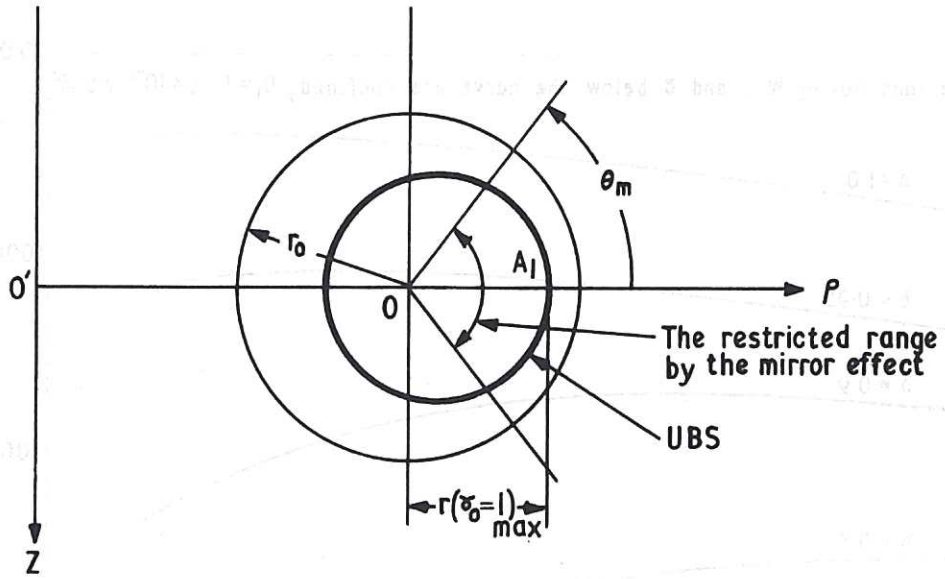

Fig. 22 (CLM-R67)
Restriction on the particle motion by the mirror effect
$\delta > \delta_L \quad \therefore r(\gamma_0 = 1)_{max} = r(\gamma_0)\,|_{\theta=0}$

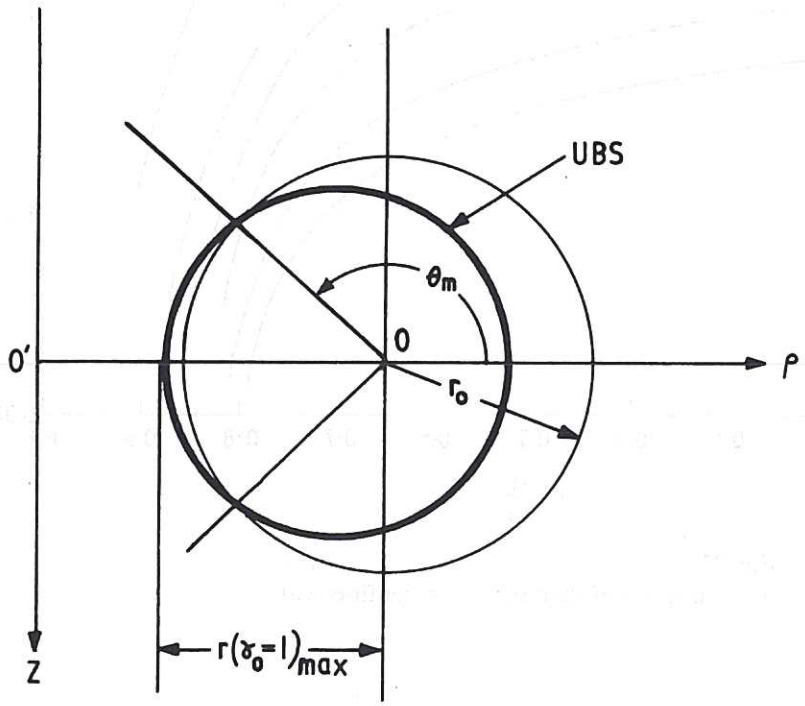

Fig. 23 (CLM-R67)
Restriction on the particle motion by the mirror effect
$\delta > \delta_L \quad \therefore \; r(\gamma_0 = 1)_{max} = r(\gamma_0 = 1)\,|_{\theta=\pi}$

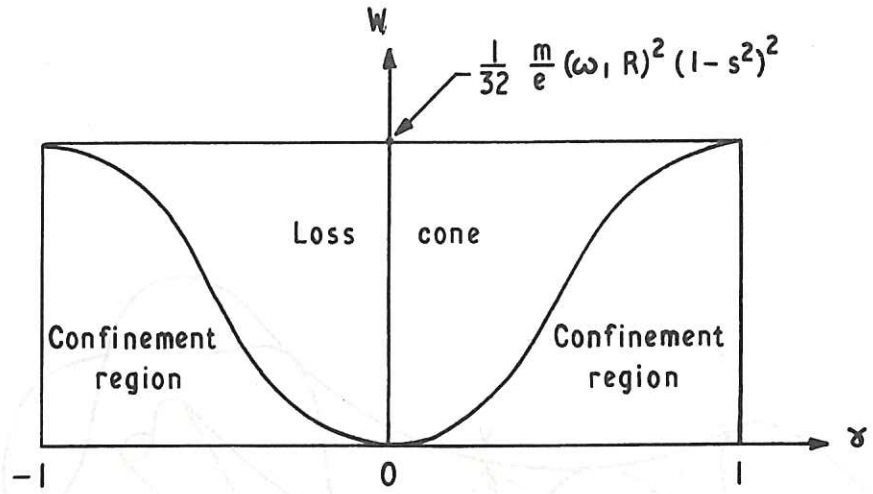

Fig. 24 (CLM-R67)
W - γ diagram in the guiding centre limit model

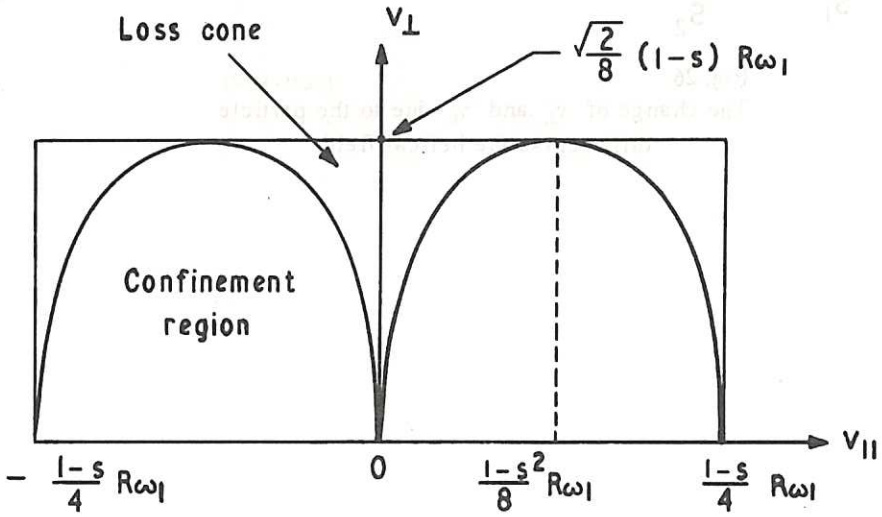

Fig. 25 (CLM-R67)
$v_\perp$ - v_{II} diagram in the guiding centre limit model

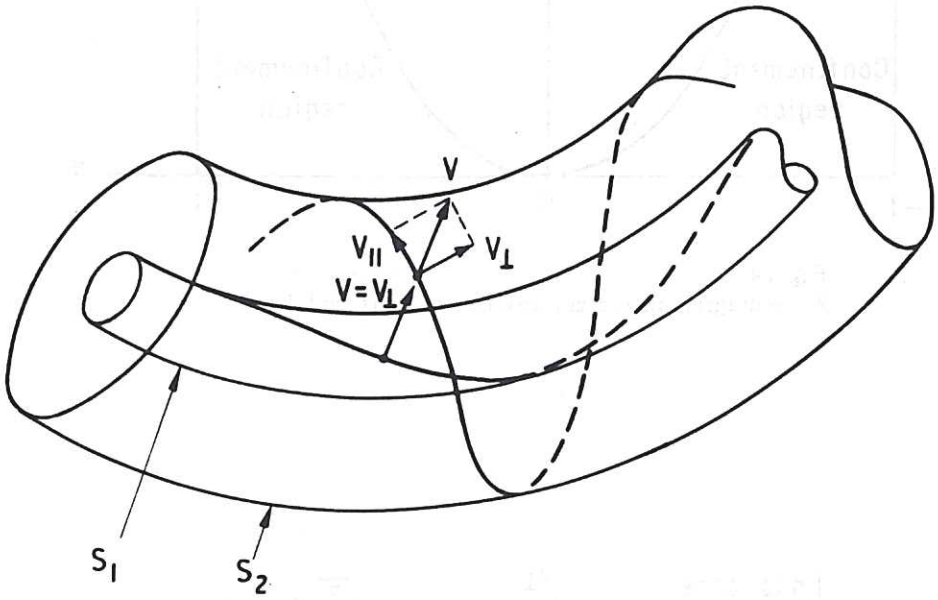

Fig. 26 (CLM-R 67)
The change of $v_{\perp}$ and $v_{\parallel}$ due to the particle drift across the helical field

Available from

HER MAJESTY'S STATIONERY OFFICE

49 High Holborn, London, W.C.1
423 Oxford Street, London W.1
13a Castle Street, Edinburgh 2
109 St. Mary Street, Cardiff
Brazennose Street, Manchester 2
50 Fairfax Street, Bristol 1
35 Smallbrook, Ringway, Birmingham 5
80 Chichester Street, Belfast

or through any bookseller.

Printed in England

S.O. Code No. 91-3-19.95